MODELING OF BROACHING

FOR OPTIMIZATION PURPOSES

by

ÖZKAN ÖZTÜRK

Submitted to the Graduate School of Engineering and Natural Sciences
in partial fulfillment of
the requirements for the degree of
Master of Science

Sabancı University

July 2003

MODELING OF BROACHING

FOR OPTIMIZATION PURPOSES

APPROVED BY:

Assistant Prof. Dr. Erhan Budak …….

(Thesis Advisor)

Assistant Prof. Dr. Gökhan Göktuğ …….

Assistant Prof. Dr. Tonguç Ünlüyurt …….

DATE OF APPROVAL: …….

ACKNOWLEDGEMENTS

I thank my advisor Assistant Prof. Dr. *Erhan Budak* for his guidance, motivation and encouragement.

I would like to thank Mr. D.G. McIntosh for his support throughout the development. Discussions with Dr. S. Engin have been very helpful.

I wish to thank my mother, father, brother, uncle and my small and sweet cousin *Özge* for their emotional support. They have always encouraged and supported me.

I am grateful to *Evren Burcu Kıvanç* who has helped me get through the difficult times and for all the emotional support, encouragement and comradeship. Thanks for two years we spent together.

Special thanks my old roommate *Bülent Delibaş, Çağdaş Arslan, Bilge Küçük*, *Şilan Hun and Mehmet Kayhan* who have made this thesis possible. They have assisted me during my whole study.

.

ABSTRACT

High productivity and high quality can be achieved in broaching if the process is applied properly. Roughing, semi-finishing and finishing can be performed in one stroke of the tool increasing productivity and reducing set-up time. Furthermore, high quality surface finish can be obtained due to straight motion of the tool. One big disadvantage of broaching is that all process parameters, except cutting speed, are built into broaching tools. Therefore, it is not possible to modify cutting conditions during the process once the tool is manufactured. Improved design of broaching tools needs detailed modeling and analysis of the broaching process.

In this thesis, tool optimization method and process models are presented. Cutting forces, tooth stresses, part deflections are modeled and analyzed using cutting models and FEA. The results of the analysis are summarized in analytical forms so that they can be used for different cases although in this thesis turbine disc broaching is considered as the application which is one of the most complex broaching operations. The developed models are implemented into a simulation program and the force, power, tooth stress and part deflection predictions are presented. The broach tool design is improved. Applications of the model for improved tool design are demonstrated by examples.

ÖZET

Broşlama işlemi yüksek verimlilik ve kalite elde edilebilecek bir metal işleme yöntemidir. Kaba talaş, ince talaş ve yüzey bitirme işlemleri tek strokta yapılabildiği için takım ve iş parçası bağlama zamanını azaltır ve yüksek verimlilik sağlar. Broş tığının dönmek yerine düz hareket etmeside iyi derecede yüzey kalitesi elde edilmesinin bir sonucudur. Broşlama işleminin en büyük dezavantajı kesme hızı dışındaki diğer kesme koşulları tamamıyla broş tığının tasarımına bağımlıdır. Broş tığı tasarlandıktan sonra kesme koşullarını değiştirmek ancak yeni bir tasarım ile mümkündür. Bu sebepten dolayı broşlama işleminin modellenmesi ve analiz edilmesi, broş tığlarının geliştirilmesi için çok gerekli bir işlemdir.

Bu tezde, broş işleminin modellenmesi ve iyileştirilmesi yapılmıştır. Kesme kuvvetleri, dişlerde oluşan gerilmeler, parça deformasyonları kesme modelleri ve sonlu elemanlar metodu kullanılarak modellenmiş ve analiz edilmiştir. Bu analizler sonucu elde edilmiş olan genel denklemler, örnek olarak zor bir işlem olarak bilinen türbin disklerinde bulunan formların üretilmesinde uygulanmıştır. Elde edilen modeller bir simulasyon programı yazılarak kesme kuvvetleri, gücü, dişlerde olusan gerilmeleri ve parça deformasyonlarını tahmin etmekte kullanılır. Bu tahminler ayni zamanda tığda nasıl iyilestirmeler yapılabileceği konusunda yardımcı olur. Bu uygulamalar örneklerle desteklenmiştir.

TABLE OF CONTENTS

LIST OF FIGURES

LIST OF TABLES

MODELING OF BROACHING

FOR OPTIMIZATION PURPOSES

by

ÖZKAN ÖZTÜRK

Submitted to the Graduate School of Engineering and Natural Sciences
in partial fulfillment of
the requirements for the degree of
Master of Science

Sabancı University

July 2003

MODELING OF BROACHING

FOR OPTIMIZATION PURPOSES

APPROVED BY:

Assistant Prof. Dr. Erhan Budak …….

(Thesis Advisor)

Assistant Prof. Dr. Gökhan Göktuğ …….

Assistant Prof. Dr. Tonguç Ünlüyurt …….

DATE OF APPROVAL: …….

ACKNOWLEDGEMENTS

I thank my advisor Assistant Prof. Dr. *Erhan Budak* for his guidance, motivation and encouragement.

I would like to thank Mr. D.G. McIntosh for his support throughout the development. Discussions with Dr. S. Engin have been very helpful.

I wish to thank my mother, father, brother, uncle and my small and sweet cousin *Özge* for their emotional support. They have always encouraged and supported me.

I am grateful to *Evren Burcu Kıvanç* who has helped me get through the difficult times and for all the emotional support, encouragement and comradeship. Thanks for two years we spent together.

Special thanks my old roommate *Bülent Delibaş, Çağdaş Arslan, Bilge Küçük*, *Şilan Hun and Mehmet Kayhan* who have made this thesis possible. They have assisted me during my whole study.

.

ABSTRACT

High productivity and high quality can be achieved in broaching if the process is applied properly. Roughing, semi-finishing and finishing can be performed in one stroke of the tool increasing productivity and reducing set-up time. Furthermore, high quality surface finish can be obtained due to straight motion of the tool. One big disadvantage of broaching is that all process parameters, except cutting speed, are built into broaching tools. Therefore, it is not possible to modify cutting conditions during the process once the tool is manufactured. Improved design of broaching tools needs detailed modeling and analysis of the broaching process.

In this thesis, tool optimization method and process models are presented. Cutting forces, tooth stresses, part deflections are modeled and analyzed using cutting models and FEA. The results of the analysis are summarized in analytical forms so that they can be used for different cases although in this thesis turbine disc broaching is considered as the application which is one of the most complex broaching operations. The developed models are implemented into a simulation program and the force, power, tooth stress and part deflection predictions are presented. The broach tool design is improved. Applications of the model for improved tool design are demonstrated by examples.

ÖZET

Broşlama işlemi yüksek verimlilik ve kalite elde edilebilecek bir metal işleme yöntemidir. Kaba talaş, ince talaş ve yüzey bitirme işlemleri tek strokta yapılabildiği için takım ve iş parçası bağlama zamanını azaltır ve yüksek verimlilik sağlar. Broş tığının dönmek yerine düz hareket etmeside iyi derecede yüzey kalitesi elde edilmesinin bir sonucudur. Broşlama işleminin en büyük dezavantajı kesme hızı dışındaki diğer kesme koşulları tamamıyla broş tığının tasarımına bağımlıdır. Broş tığı tasarlandıktan sonra kesme koşullarını değiştirmek ancak yeni bir tasarım ile mümkündür. Bu sebepten dolayı broşlama işleminin modellenmesi ve analiz edilmesi, broş tığlarının geliştirilmesi için çok gerekli bir işlemdir.

Bu tezde, broş işleminin modellenmesi ve iyileştirilmesi yapılmıştır. Kesme kuvvetleri, dişlerde oluşan gerilmeler, parça deformasyonları kesme modelleri ve sonlu elemanlar metodu kullanılarak modellenmiş ve analiz edilmiştir. Bu analizler sonucu elde edilmiş olan genel denklemler, örnek olarak zor bir işlem olarak bilinen türbin disklerinde bulunan formların üretilmesinde uygulanmıştır. Elde edilen modeller bir simulasyon programı yazılarak kesme kuvvetleri, gücü, dişlerde olusan gerilmeleri ve parça deformasyonlarını tahmin etmekte kullanılır. Bu tahminler ayni zamanda tığda nasıl iyilestirmeler yapılabileceği konusunda yardımcı olur. Bu uygulamalar örneklerle desteklenmiştir.

TABLE OF CONTENTS

LIST OF FIGURES

LIST OF TABLES

CHAPTER 1 INTRODUCTION

Broaching is commonly used in industry for the machining of variety of external or internal features such as keyways, noncircular holes, fir-tree slots on turbine discs etc. The tool used for broaching is called *broach.* A broach has many teeth on it. Each has a slightly higher height than the previous one (Figure 1-1 & Figure 1-2). The peripheral shape of the broach is the inverse of the final shape of the profile to be machined.

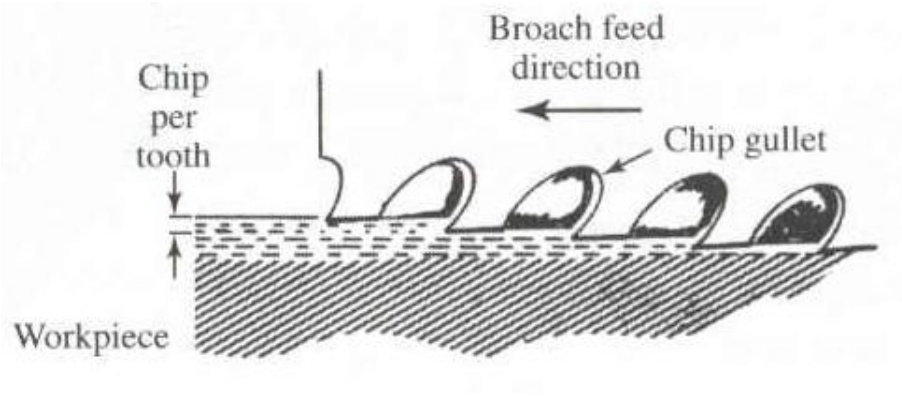

Figure 1-1: Basic broaching process view.

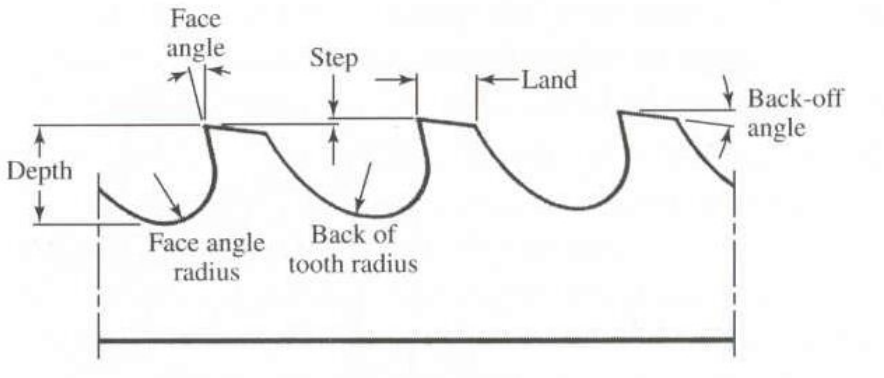

Figure 1-2: Tooth profile.

Mostly, a broach tool has three sections on it which are called roughing, semi-finishing and finishing (Figure 1-3). Roughing teeth are suscept to higher chip load than finishing teeth. Since grinding the broach teeth is a difficult process, some teeth have equal height in finishing section in case teeth wear. The teeth start to wear from the first teeth to the last.

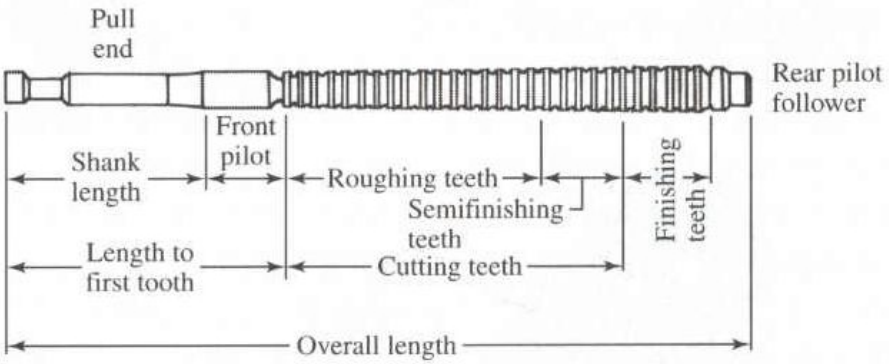

Figure 1-3: Complete broach tool.

Broaching can offer very high productivity and part quality when the conditions are selected properly. It has several advantages over other machining processes. Most important of them being roughing and finishing of a complex form on a part can be completed in one stroke of the machine without the need of skilled labour which would require many passes with another process such as milling. Also, straight and non-rotating tool motion results in good surface finish without feed marks. However, achieving high quality and productivity continuously in production needs a well-designed process. In broaching, all process parameters except cutting speed are defined by the broach. Therefore, it is not possible to modify cutting conditions after teeth are manufactured unlike other machining processes where depth-of-cut or feedrate can be changed easily. This makes tool design the single most important aspect of broaching.

1.1 Literature Survey

The removal of the metal from the workpiece is called *machining*. Machining processes such as *turning*, *milling* and *drilling* are the most common applications. There are also special applications such as *broaching*, *boring*, *hobing*, *shaping*, and *grinding*. Although they have different kinematics and geometry, the mechanics of all based on the same principles depend on the process.

F.W. Taylor is the great historical figure in the field of metal cutting. Taylor's most important practical contribution was his invention, with White, of high speed steel cutting tools. Taylor's most important research contribution was his famous tool life equation after his recognition of the importance of tool temperatures in tool life. He summarized his contributions in [1]. A great deal of research in metal cutting has been conducted since 1900.

Armarego and Brown [2], Shaw [3] and Oxley [4] present models and methods related to the analysis of mechanics of cutting. Altintas [5] also presents similar analysis for the mechanics of metal cutting for machining processes such as milling, turning and drilling in detail. Trent and Wright [6] and Childs et al. [7] presented results of their studies on machining.

Merchant [8] developed an orthogonal cutting model by assuming the shear zone to be a thin plane. He applied minimum energy principle to orthogonal cutting in order to develop an equation for shear angle. Also, Lee and Shaffer [9] and Palmer and Oxley [10] proposed their shear angle prediction models by using laws of plasticity. Krystof [11] proposed a shear angle relation based on maximum shear stress principle. They both assumed that shear occurs in the direction of maximum shear stress.

The earliest finite element analyses application on chip formation was done by Zienkiewwicz [12] and Kakino [13]. They modeled large flows by simulating the loading of a tool against a pre-formed chip. This study has some assumptions such as

neglecting the friction between the chip and tool, and strain rate and temperature material flow stress variations. These assumptions are considered in the study of Shirakashi and Usui [14]. They developed an iterative way of changing the shape of the pre-form until the generated plastic flow was consistent with assumed shape. Iwata et al. [15] applied the steady state rigid-plastic modeling, within a Eulerian framework, also adjusting an initially assumed flow field to bring it into aggrement with the computed field. Friction and work hardening are also included to the model.

As the computation power increases the updated Lagrangian elastic-plastic analysis was used, and chip/workpiece separation criterion at the cutting edge becomes the main point to consider. Strenkowski and Carrol [16] used strain based separation criterion. Three dimensional elastic-plastic, thermally coupled, iterative convergence method simulation is used for cutting tool design by Maekawa et al. [17]. The rigid-plastic method of Iwata was developed by Ueda and Manabe [18] and Ueda and et al. [19] with using Lagrangian modeling instead of Eulerian. Adaptive remeshing was applied to chip formation simulations by Sekhon and Chenot [20] and Ceretti [21] to rigid-plastic and by Marusich and Ortiz [22].

Although widely used in industry, there is very limited literature on broaching. The book by Monday [23] presents the technology of broaching machines, processes and tools in a detailed manner. Although this is relatively an old reference, most of the material in the book still applies to current broaching operations. Collection of the works edited by Kokmeyer [24] has several different broaching applications in industry demonstrating the effectiveness of the process. Terry et al. [25] presented a knowledge based system approach that can be used in design of broaching tools. Gilormini et al. [26] analyzed the cutting forces on a single broaching section and compared them with the forces in tapping and slotting. Sutherland et al. [27] demonstrated the application of a mechanistic force model to gear machining. In one of the recent works, Sajeev et al. [28] presented the finite element analysis results for the effects of burnishing in broaching. Last section of a broach set usually burnishes the surface to improve surface finish and surface integrity. The analysis done by Sajeev et al. [28] is interesting to understand the mechanics of this process. Taricco [29] presented the tool wear affects on the surface integrity of the broached slots which increases the risk of high tensile stresses on the surface. Also, the power monitoring results of a fir-tree profile

production on turbine discs by Budak [30] are very helpful for identification of the possible improvements on the tool design.

Optimization problem of a machining process has been researched for decades. Several optimization techniques applied to machining problems. Bhattacharyya et al. [31] used Lagrangian method, Ermer [32] used geometric programming, Satyanarayana et al. [33] used goal programming, Arsecularathane et al. [34] used direct search method, Mesquita et al.[35] used non-linear programming, Khan et al. [36] used genetic algorithms and Alberti and Perrone [37] used fuzzy logic and genetic algorithms.

1.2 Problem Definition

Tool design is the most important criteria since there is no any other flexibility in the process. Only the cutting speed can be changed after a broach is designed and manufactured. Therefore, proper design of broach tools is utmost important. Modeling cutting process and predicting important parameters before the design stage will be very helpful for optimum tool design.

Current broach designs do not completely depend on a scientific base. They are usually based on experience. Since there is not much literature about broaching, the broach design and the process mostly depend on the experience of the designer. There is no model for the optimal tool design. This may result in lost time, reduced quality and increased cost. Current broach design can be improved by process models. For example, tool length can be shortened and the process time is reduced, tooth breakage can be prevented, part quality can be improved etc. Some modifications can also be done on pitch, chip load and tooth profile.

The main objective of this study is to apply models such as force, power, tooth stress and part quality in order to improve broach tool design. As an example application, fir-tree form which is one of the most difficult profile machined by broaching is used in the thesis. Also the material used in this application –waspaloy- is one of the hardest materials to machine. The models obtained in this study can be extended to other applications of broaching.

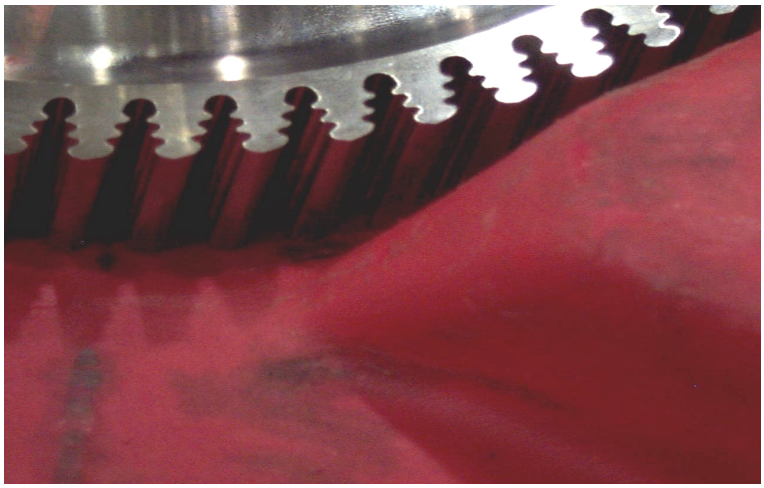

Figure 1-4: Fir-tree profile on turbine discs.

Machining of fir-tree forms (Figure 1-4) on turbine discs is regarded as one of the most difficult broaching operations due to complex geometry and very tight tolerances. The material used in turbine discs is Waspaloy. Waspaloy is a difficult-to-machine nickel based superalloy work material used in turbine compressor blades and discs, shafts, spacers, fasteners, miscellaneous jet engine hardware; space shuttle turbo pump seals due to its strength at elevated temperatures. The continual need for greater thrust output and better fuel efficiency has resulted in faster-spinning, hotter-running gas turbine engines. This, in turn, has created the need for alloys that can withstand higher stresses and temperatures. Another critical material property is the ability to resist corrosion at ambient and elevated temperatures, including general corrosion, crevice corrosion, stress corrosion, oxidation and sulfidation. Superalloys like waspaloy meet the mechanical strength requirements like tensile, shear, fatigue, creep and/or stress rupture strengths, high temperatures and corrosion resistance.

The broach used for fir-tree profile production consists of several sections as shown in Figure 1-5. Generally, the first five or six sections are used for roughing. Then the fir-tree profile is started to be formed by roughing. The upper part of the fir-tree profile is a problematic section of the profile to machine. Tooth thickness just below the section decreases because of the neck. In these sections the tooth rise (chip load) is kept small to prevent breakage. Also in final finishing sections, the rise per tooth is very small, moreover there are teeth with no rise which remove the left over material due to worn teeth.

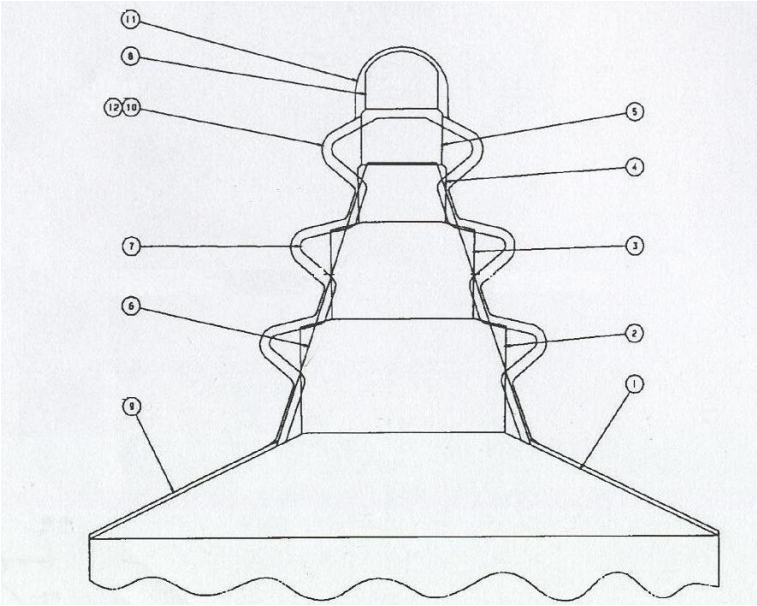

Figure 1-5: Tooth forms for different sections on a broaching tool set.

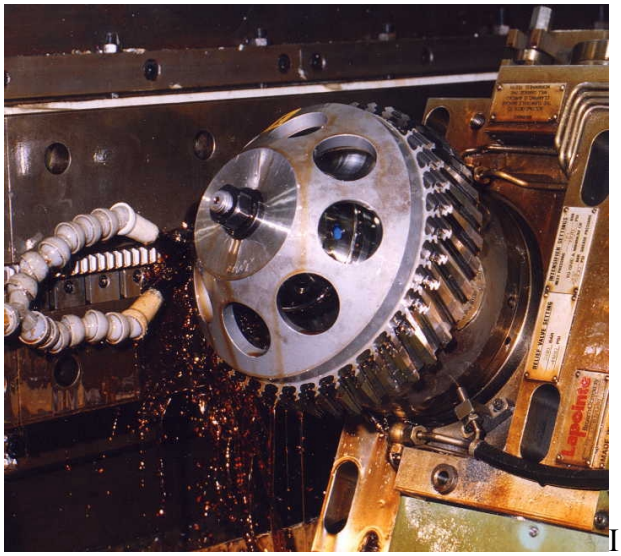

Figure 1-6: Broaching of fir-tree forms on a turbine disc.

There is not much experimental cutting data available for waspaloy. For this reason, it is hard to develop a force model and force model related models.

1.3 Methodology

First of all, there is a need for a force model for HSS-T tool and waspaloy material combination. There can be several approaches such as analytical models, FEA based modeling and emperical methods which will be discussed in detail later. In analytical model, orthogonal cutting formulations will be used. FEA simulations of broaching will be used for FE based modeling. Some orthogonal cutting tests will be performed and experimental model will be obtained.

Based on the developed force model, other relevant models will be formulated. Since broaching is a process that requires high power, the power drawn during the process has to be calculated. Chatter stability will be considered for broaching using orthogonal stability limit formulations. Minimum and maximum chip load should be specified as a constraint for the process in order to prevent rubbing and chipping observed in practice. A practical broach life must be selected based on the previously obtained life data.

The next step after process modeling is creation of the structural models. Structural analysis include broach tooth stresses, part deflection for quality considerations etc. An important problem is tooth breakage during the process which needs to be predicted and prevented. The FE method will be used to create a model for the tooth. Tooth geometry will be generalized and tooth geometry parameters will be changed gradually. An equation can be derived for stress based on these results. The part quality is another important issue in broaching. During broaching, work material deflects because of the cutting forces, and this causes form errors on the final part. In order to predict how much workpiece deflects according to number of teeth in cut, teeth positions, and the workpiece geometry, some FEA will be carried out by changing those parameters as in tooth stress analysis, and an equation can be generated. If the chip space between two teeth is not enough, the accumulated chip may get stuck in the chip space and increase the cutting load. For that reason, the amount of chip in the space

must be controlled. The chip space according to the dimensions of the tooth needs to be calculated and compared with the chip volume. Available ram length should also be considered in the broach design. It is also important to set a limit to force fluctuation within a section or from section to section. High fluctuations mean more impact imposed on the tool and may cause fatigue failure.

After developing the process and structural models, they will be integrated in a program written in Matlab[1]. Based on the simulation results, the modifications and improvements needed on the broach design are determined

[1] Matlab is a trademark of The MathWorks, Inc

CHAPTER 2 PROCESS MODELING

Process modeling is the first step of defining the broaching process. This chapter will introduce the models developed for broaching with details.

2.1 Force Model

The main requirement for prediction of the results of a machining process is the force prediction. The cutting forces can be used for predicting the power drawn during the process, the stresses on the broach tools, and the form errors on the part. The directions of the cutting forces depend on the geometry of tool and the direction of cut. In an orthogonal cutting the exerted forces are only in two directions as seen on Figure 2-1. The first one is tangential cutting force (F_t) which is in the direction of the movement of tool relative to the workpiece, the other one is the feed force in the direction of the chip thickness (F_f). But in oblique cutting another force component exerted on the tool in the third direction called radial cutting force (F_r) as shown on Figure 2-2. In broaching process mostly the tools are designed for orthogonal cuts since it is hard to design the tool for oblique cutting and also it increases the cutting length.

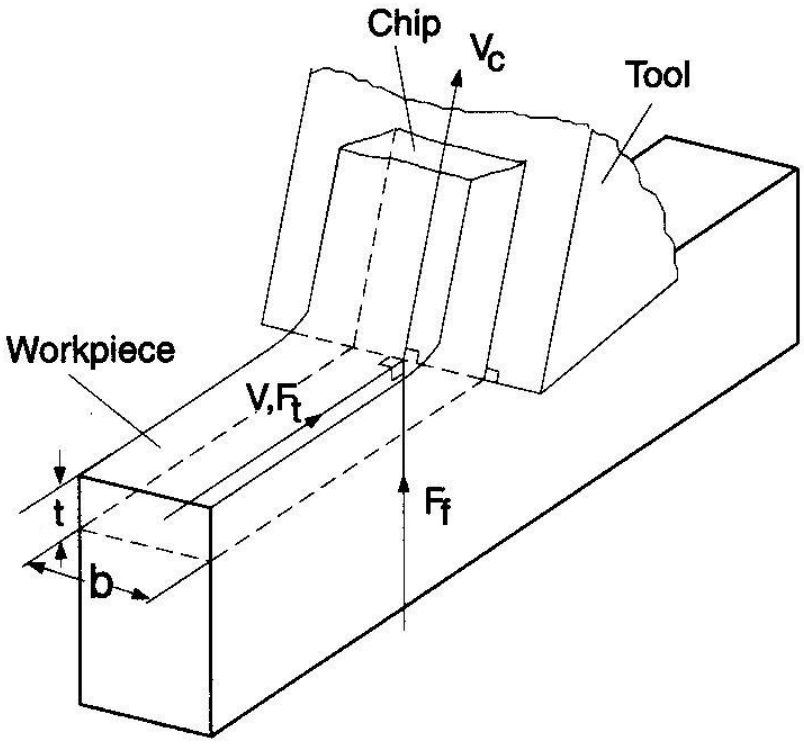

Figure 2-1: Cutting Forces Orthogonal Cutting.

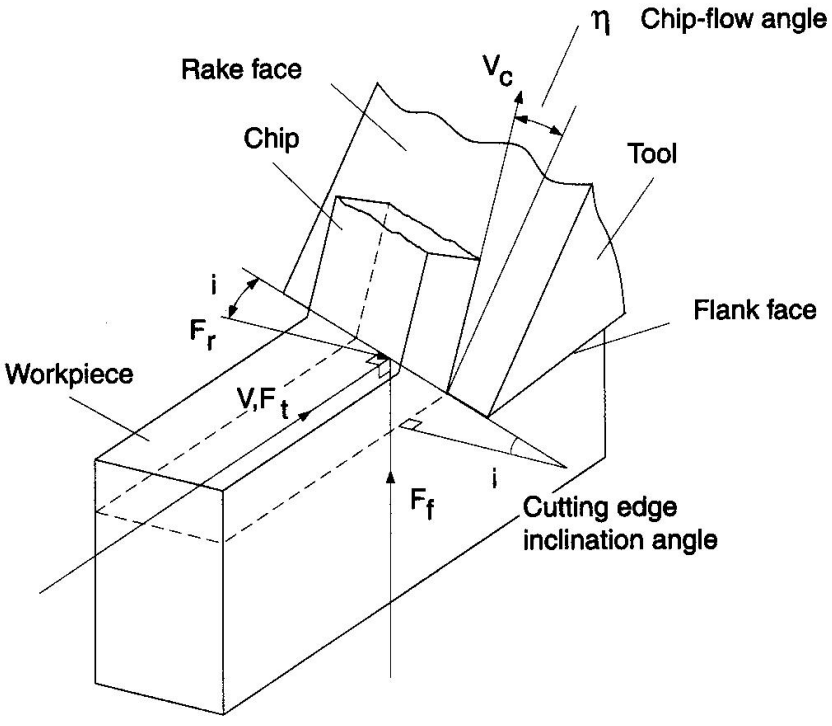

Figure 2-2: Cutting Forces in Oblique Cutting.

The cutting forces can be calculated by using the chip area sheared away from the workpiece and cutting force coefficients. The chip area is calculated by multiplying width of cut (b) and depth of cut (t).

$$F_i = K_i bt \tag{2.1}$$

where K is the force coefficient and i indicates the direction of force (feed or tangential).

The cutting coefficients depend on the tool and the workpiece material combination. For different tool material and workpiece combinations the cutting forces will differ. The easiest way to determine the cutting force coefficients is using orthogonal cutting models. If an oblique model is needed, the orthogonal cutting data can be used to predict the forces in oblique cutting [38] .

In general, broaching is an orthogonal cutting process. In some cases, cutting teeth may have an inclination angle to provide a smooth entry and exit to and from the cut making the process oblique. The data from other cutting processes cannot be used for broaching due to extremely small cutting speeds. There are several ways to identify the orthogonal cutting force coefficients.

2.1.1 Analytical Model

The cutting force coefficients could be calibrated as in the mechanistic models which needs force measurements. However, instrumentation of broaching machines is very difficult as they do not have tables for clamping a dynamometer. For this reason analytical modeling can be used for predictions.

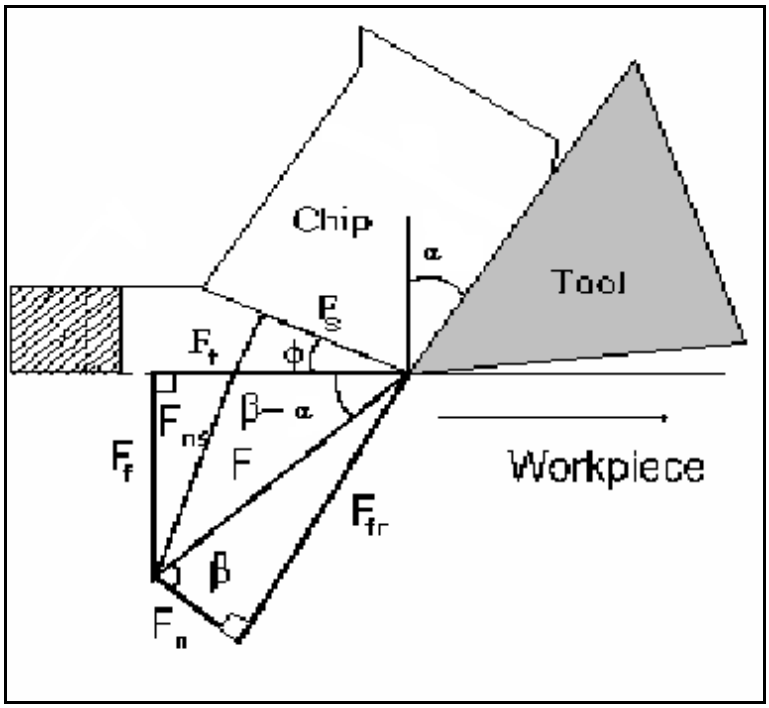

Figure 2-3: Cutting Force Diagram.

In this model analytical formulations for cutting force coefficients in orthogonal cutting are used as in [2]:

$$K_t = \left[\tau_s \frac{\cos(\beta - \alpha)}{\sin(\phi)\cos(\phi + \beta - \alpha)} \right]$$
$$K_f = \left[\tau_s \frac{\sin(\beta - \alpha)}{\sin(\phi)\cos(\phi + \beta - \alpha)} \right] \qquad (2.2)$$

where K_t and K_f are the cutting force coefficients in the cutting and feed (normal) directions, τ_s is the shear stress in the shear plane. $\varnothing$, β and α are the shear, friction and rake angles, respectively (Figure 2-3). These parameters can be experimentally identified. However, if there is no experimental data available, tabulated values can be used. Shear angle can be predicted by Minimum energy principle proposed by Merchant [8].

$$\phi = \frac{\pi}{4} - \frac{(\beta - \alpha)}{2} \qquad (2.3)$$

Rake angle is dependent on tool geometry and the friction angle is also tool and workpiece material dependent. The friction angles are generally around 30^o and 40^o.

Example 2-1 Calculation of Analytical Force Coefficient for Waspaloy

Cutting tool geometry:

Rake Angle(α): 12^o

Material Properties:

Shear Stress(τ_s): 1250 MPa

Friction Angle (β): 35^o

By using Equation (2.3)

Shear Angle: $\phi = \frac{\pi}{4} - \frac{(\beta - \alpha)}{2} = 45 - \frac{(35-12)}{2} = 33.5^o$

Put shear angle, shear stress, rake and friction angle into Equation (2.2)

$$K_t = \left[\tau_s \frac{\cos(\beta - \alpha)}{\sin(\phi)\cos(\phi + \beta - \alpha)} \right] = 1250 \frac{\cos(35-12)}{\sin(33.5)\cos(33.5+35-12)} = 3777 N/mm^2$$

$$K_f = \left[\tau_s \frac{\sin(\beta - \alpha)}{\sin(\phi)\cos(\phi + \beta - \alpha)} \right] = 1250 \frac{\sin(35-12)}{\sin(33.5)\cos(33.5+35-12)} = 1603 N/mm^2$$

2.1.2 Finite Element Analyses Model

When experimental data is not available, another method using finite element analyses can be useful. There are several commercial softwares for machining simulations such as AdvantEdge[2] and DEFORM[3]. Some tests are performed on Third Wave AdvantEdge Software. Advantage is a two-dimensional Lagrangian finite element software package for machining modeling. The FEA simulation results heavily depend on the material flow model which is usually not very accurate for the conditions of metal cutting The material model of the software contains power strain-hardening, thermal softening and rate sensitivity laws. Heat generation and transfer are handled via the second law of thermodynamics. AdvantEdge uses a six-noded quadratic triangle (Figure 2-4) element for the spatial discretization. The element has three corner and three midside nodes providing quadratic interpolation of the displacements within the element. During metal cutting the workpiece material is allowed to flow around the cutting tool edge. In this vicinity, elements periodically will become much more distorted and lose accuracy. The software updates the finite element mesh by refining large elements, remeshing distorted elements, and coarsening small elements (Figure 2-5).

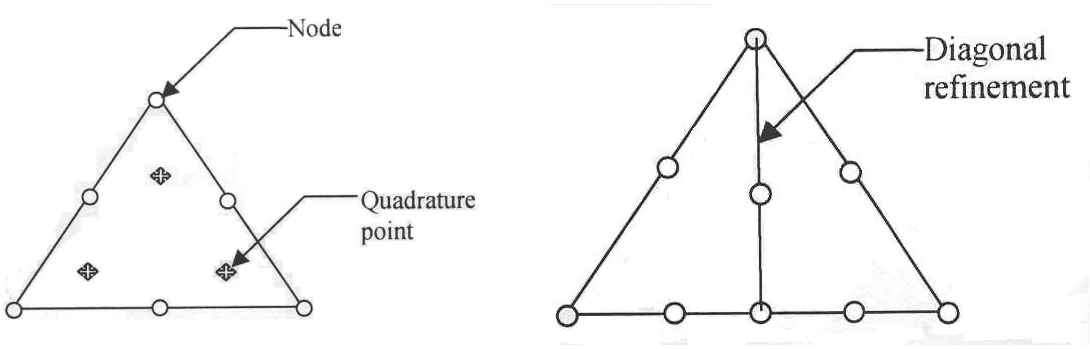

Figure 2-4: Element Type in AdvantEdge.

[2] AdvantEdge is machining simulation software of Third Wave Systems Inc.
[3] Deform is the design environment for forming software of Scientific Forming Technologies Corporation

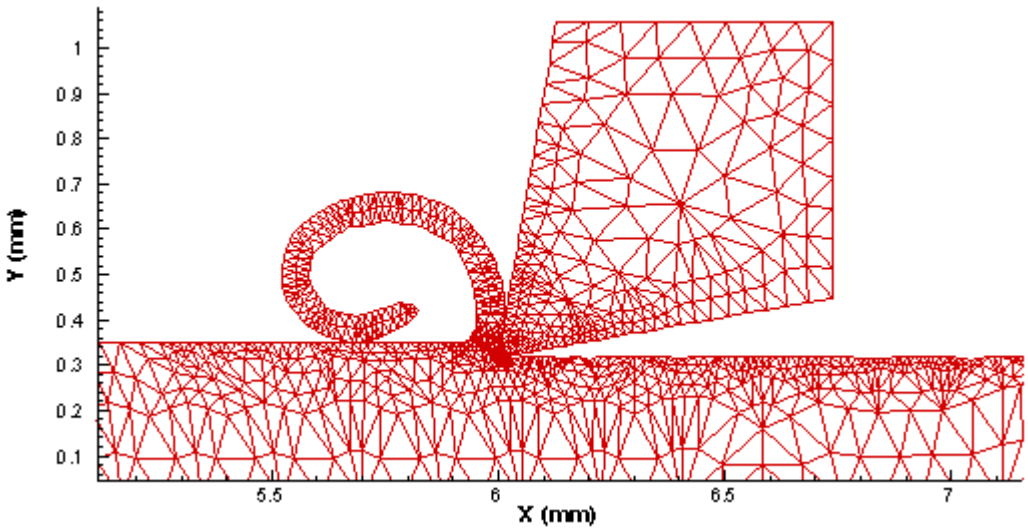

Figure 2-5: Meshing of the tool and the workpiece.

Since the aim is to form a model, the effect of process parameters (rake angle α, tool tip radius h_r, cutting speed V and chip load t) are investigated by changing them progressively. A test matrix is formed as in Table 2-1

	Rake Angle (°) α	Cutting Edge Radius (mm) h_r	Chip Load/tooth (mm) t	Cutting Speed (m/min) V
Test 1	10	0,02	0,03	3
Test 2	10	0,02	0,05	3
Test 3	10	0,02	0,1	3
Test 4	10	0,02	0,125	3
Test 5	5	0,005	0,01	6
Test 6	5	0,005	0,03	6
Test 7	5	0,005	0,05	6
Test 8	5	0,005	0,1	6
Test 9	10	0,005	0,01	6
Test 10	10	0,005	0,03	6
Test 11	10	0,005	0,05	6
Test 12	10	0,005	0,1	6
Test 13	10	0,01	0,03	6
Test 14	10	0,01	0,05	6
Test 15	10	0,01	0,1	6
Test 16	10	0,01	0,125	6
Test 17	10	0,02	0,03	6
Test 18	10	0,02	0,05	6
Test 19	10	0,02	0,1	6
Test 20	10	0,02	0,125	6
Test 21	15	0,005	0,01	6
Test 22	15	0,005	0,03	6
Test 23	15	0,005	0,05	6
Test 24	15	0,005	0,1	6
Test 25	10	0,02	0,05	12
Test 26	10	0,02	0,1	12
Test 27	10	0,02	0,125	12
Test 28	10	0,02	0,05	20
Test 29	10	0,02	0,1	20
Test 30	10	0,02	0,125	20

Table 2-1: Test Matrix for FEA in AdvantEdge.

The results of analyses are investigated, tangential and feed forces are recorded and a linear force model is obtained. Linear force model is composed of two force components. One is shearing component, the other is edge forces.

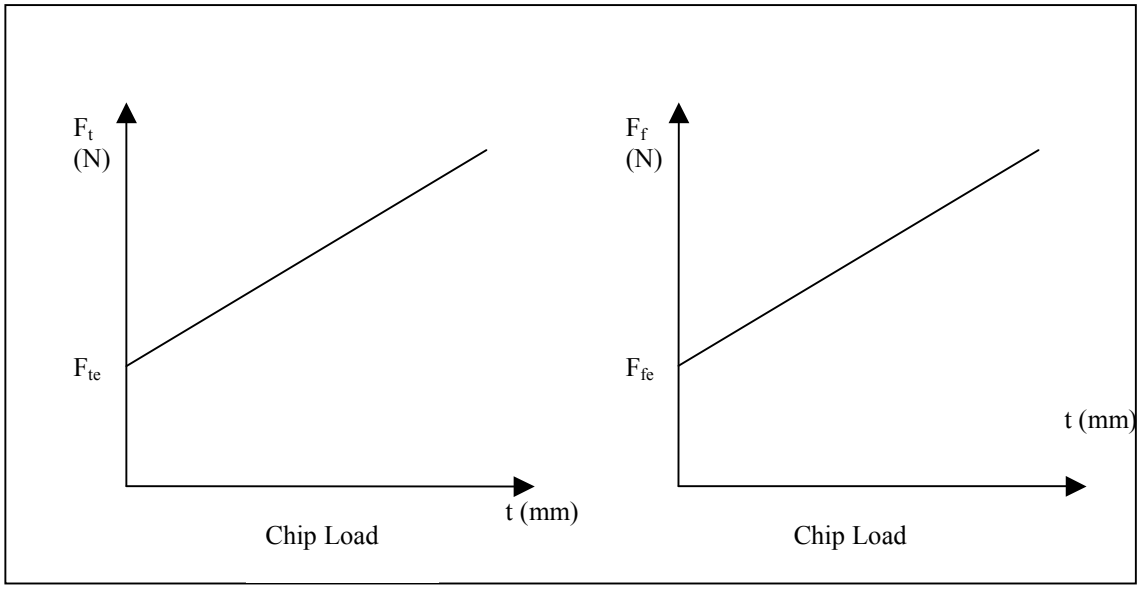

Figure 2-6: Cutting Forces vs. Chip Load.

Tangential Force:

$$F_t = F_{tc} + F_{te} \tag{2.4}$$

$$F_t = K_{tc} bt + K_{te} b \tag{2.5}$$

where K_{tc} :cutting constant, K_{te}: edge coefficient

Feed Force:

$$F_f = F_{fc} + F_{fe} \tag{2.6}$$

$$F_f = K_{fc} bt + K_{fe} b \tag{2.7}$$

where K_{fc} :cutting constant, K_{fe}: edge coefficient

The width of cut is chosen same for all cases and the obtained tangential and feed forces are fitted as in the graphs shown in Figure 2-6.

The cutting forces are read from the analyses results as follows;

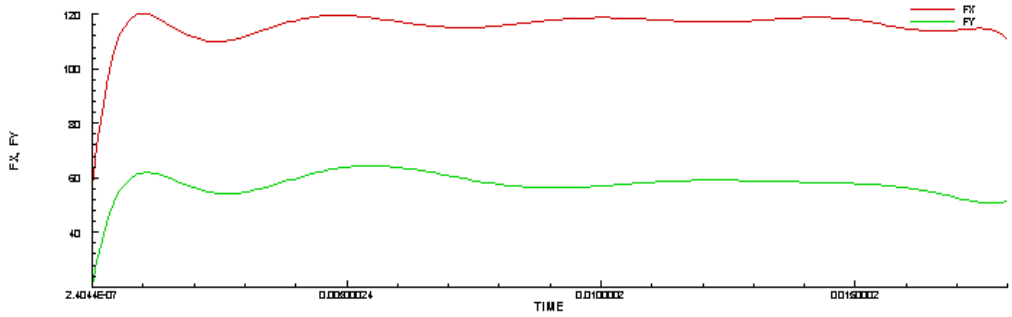

Figure 2-7: The cutting force results of an Advantage Analyses.

2.1.2.a The effect of Cutting Speed

Generally, the cutting speed in broaching is very low compared to other processes such turning and milling. Some of the tests in AdvantEdge are carried out by varying the cutting speed from 3 m/min to 20 m/min. As the chip load increases the cutting forces also increase (Figure 2-8 & Figure 2-9). K_{tc}, K_{te}, K_{fc} and K_{fe}'s are calculated and tabulated in Table 2-2.

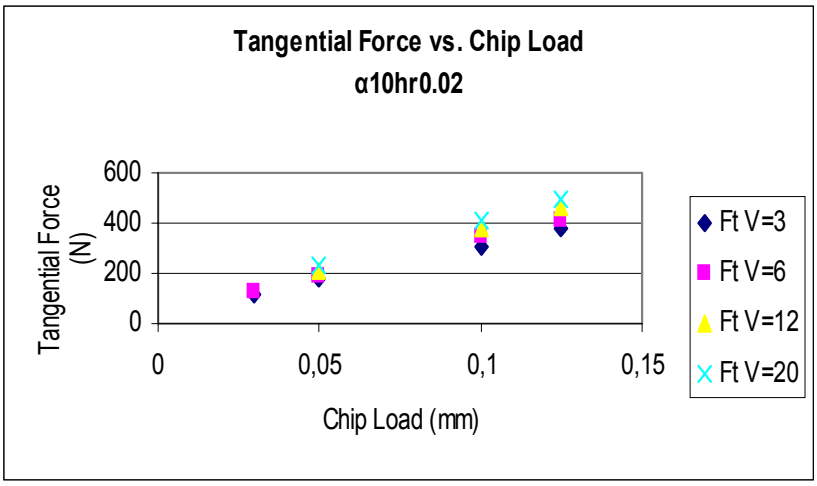

Figure 2-8: Tangential Force change by cutting speed.

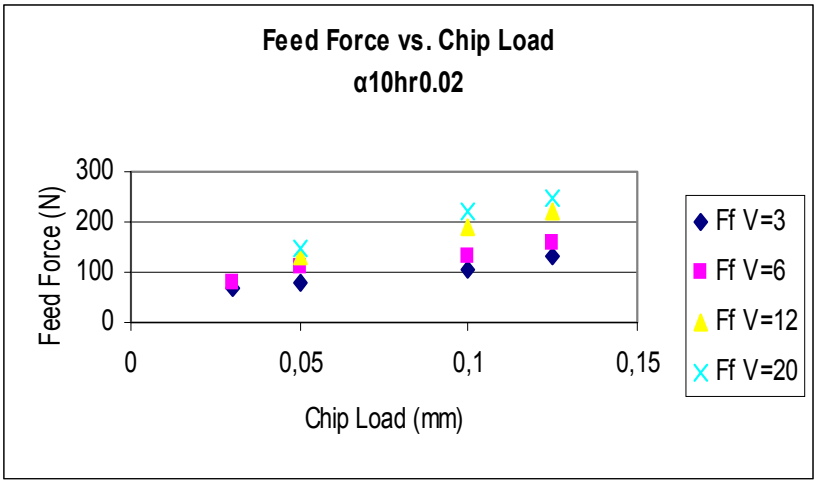

Figure 2-9 Feed Force change by cutting speed.

	Chip Load/tooth (mm) T	Cutting Speed (m/min) V	Tangential Force (N) $F_t(F_x)$	Cutting Cons (N/mm^2) K_{tc}	Edge Force Coeff (N/mm) K_{te}	Feed Force (N) $F_f(F_y)$	Cutting Cons (N/mm^2) K_{fc}	Edge Force Coeff (N/mm) K_{fe}
Test 1	0,03	3	115	2769,2	33,8	70	605,0	50,0
Test 2	0,05		175			80		
Test 3	0,1		310			105		
Test 4	0,125		380			130		
Test 17	0,03	6	130	3020,6	39,7	80	728,5	64,0
Test 18	0,05		190			110		
Test 19	0,1		345			130		
Test 20	0,125		415			158		
Test 25	0,05	12	210	3351,4	41,8	130	1200,0	70,0
Test 26	0,1		375			190		
Test 27	0,125		462			220		
Test 28	0,05	20	230	3605,7	50,1	150	1345,7	83,6
Test 29	0,1		412			221		
Test 30	0,125		500			250		

Table 2-2: Cutting speed variation text matrix.

The effect of the speed is observed in the Figure 2-10, Figure 2-11.

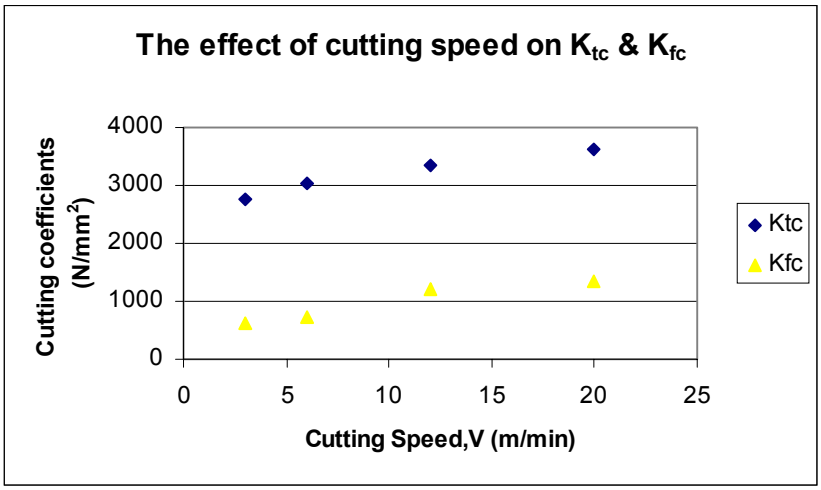

Figure 2-10: Cutting Coefficient change by cutting speed.

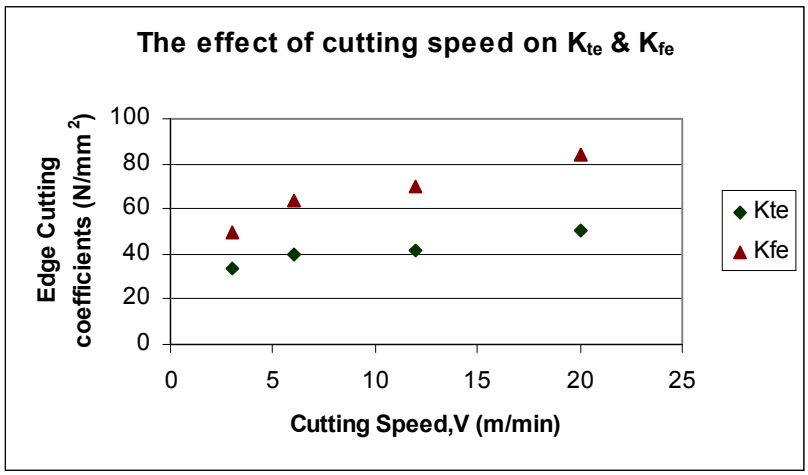

Figure 2-11 Edge Coefficient change by cutting speed.

In contrast to high speeds, the cutting coefficients increase as the speed increases. But at high speeds the coefficients decrease as the speed increases because the shear stress decreases by increasing temperature and also the friction decreases.

2.1.2.b The effect of tool tip radius

As the tool wears, the radius of the tool tip increases. Tool wear causes the increase in the cutting forces and also results in poor surface quality.

The tool tip radius is varied from 5 μm to 20 μm and the changes in the force and coefficients are observed. The results are tabulated in Table 2-3.

	Chip Load/tooth (mm) T	Cutting Edge Radius (mm) h_r	Tangential Force (N) $F_t(F_x)$	Cutting Cons (N/mm^2) K_{tc}	Edge Force Coeff (N/mm) K_{te}	Feed Force (N) $F_f(F_y)$	Cutting Cons (N/mm^2) K_{fc}	Edge Force Coeff (N/mm) K_{fe}
Test 9	0,01	0,005	44	2717,3	27,9	27	379,9	32,0
Test 10	0,03		120			51		
Test 11	0,05		169			56		
Test 12	0,1		295			66		
Test 13	0,03	0,01	125	2925,2	34,7	65	654,2	44,1
Test 14	0,05		180			75		
Test 15	0,07		235			90		
Test 16	0,1		330			110		
Test 17	0,03	0,02	130	3020,6	39,7	80	728,5	64,0
Test 18	0,05		190			110		
Test 19	0,1		345			130		
Test 20	0,125		415			158		

Table 2-3: Tool tip radius variation text matrix.

The increase in the tool tip radius causes the increase in forces and coefficients as in Figure 2-12 - Figure 2-15

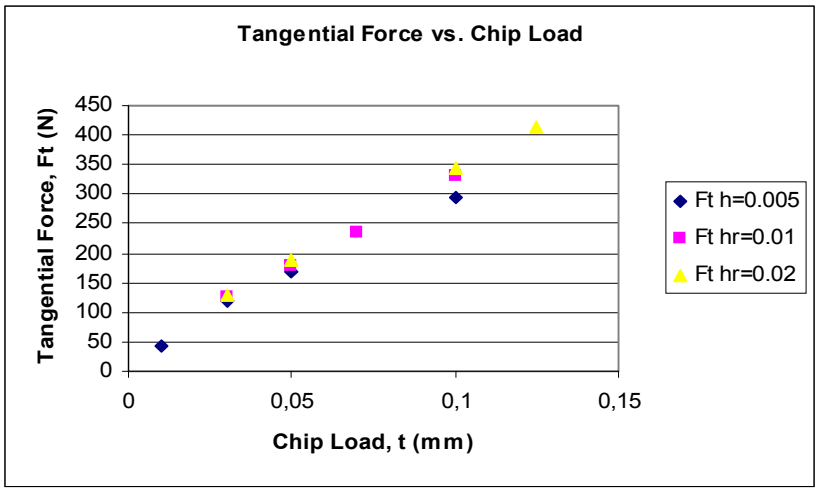

Figure 2-12: Tangential Force vs Chip Load.

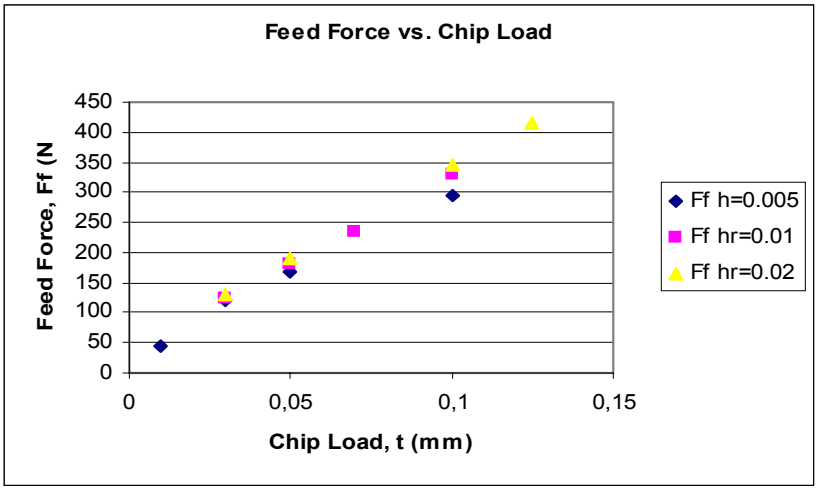

Figure 2-13: Feed Force vs Chip Load.

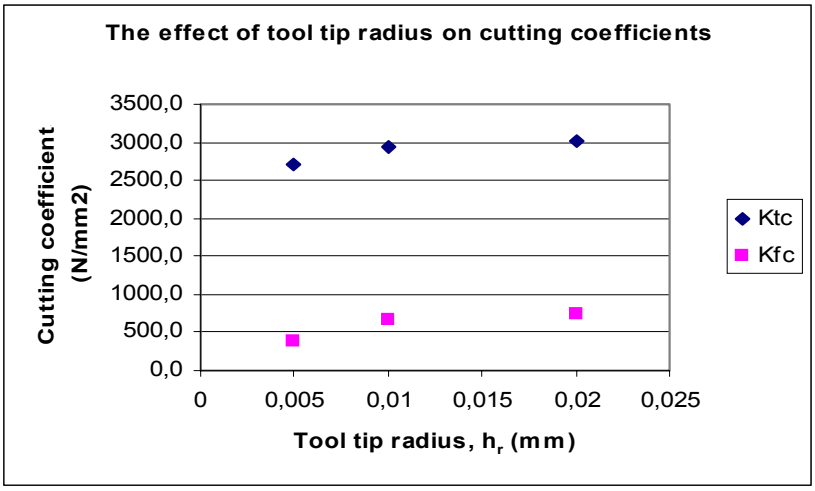

Figure 2-14: Cutting coefficient change by tool tip radius.

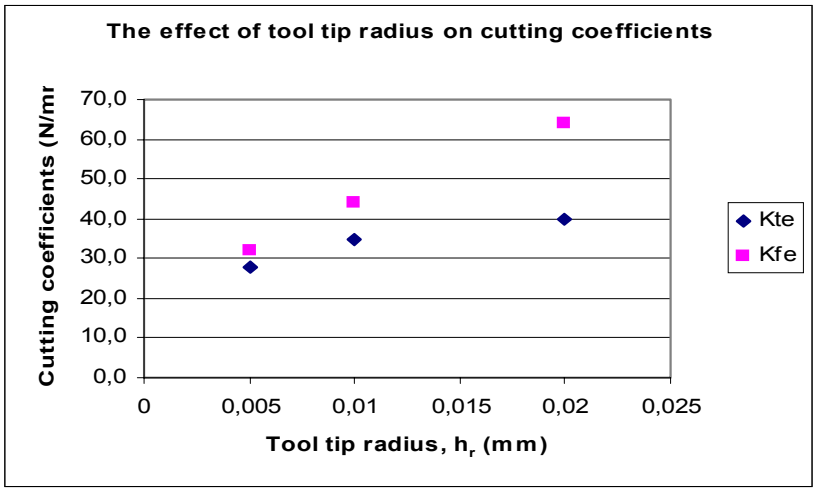

Figure 2-15: Edge coefficient change by tool tip radius.

2.1.2.c The effect of Rake Angle

The rake angle is another factor that varies the force and coefficients. The rake angle is changed between 5 degrees and 15 degrees in the analyses. It is observed that as the rake angle increases the forces and coefficients decrease but it is important to remember that the tool weakens in this case.

	Rake Angle (°) α_r	Chip Load/tooth (mm) t	Tangential Force (N) $F_t(F_x)$	Cutting Cons (N/mm^2) K_{tc}	Edge Force Coeff (N/mm) K_{te}	Feed Force (N) $F_f(F_y)$	Cutting Cons (N/mm^2) K_{fc}	Edge Force Coeff (N/mm) K_{fe}
Test 5	5	0,01	45,9	2790,8	30,9	35	558,4	33,9
Test 6		0,03	128			54		
Test 7		0,05	175			65		
Test 8		0,1	305			87,5		
Test 9	10	0,01	44	2717,3	27,9	27	379,9	32,0
Test 10		0,03	120			51		
Test 11		0,05	169			56		
Test 12		0,1	295			66		
Test 21	15	0,01	41	2638,5	24,4	24,5	250,6	28,2
Test 22		0,03	110			40		
Test 23		0,05	165			46		
Test 24		0,1	283			50		

Table 2-4: Rake Angle variation test matrix.

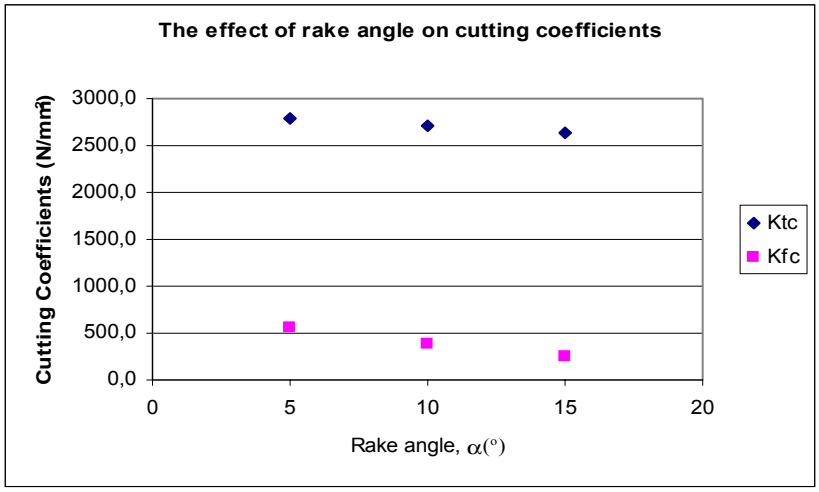

Figure 2-16 The cutting coefficient change by rake angle.

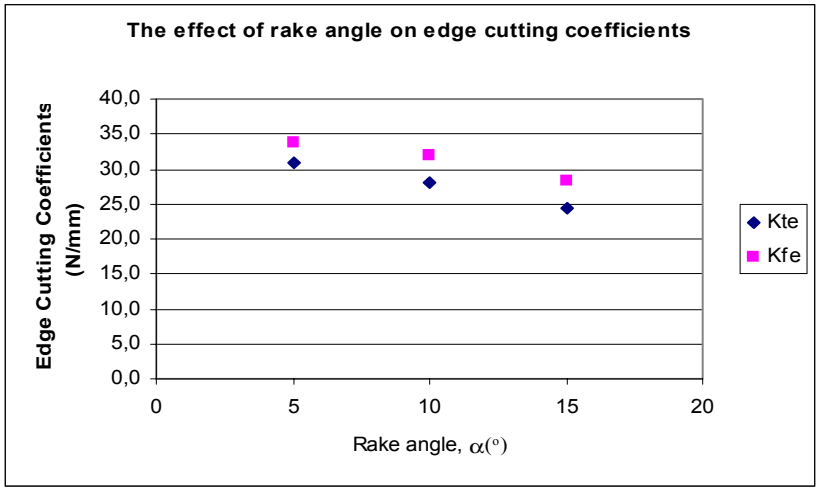

Figure 2-17 The edge cutting coefficient change by rake angle.

	Rake Angle (°) α_r	Cutting Edge Radius (mm) h_r	Chip Load/tooth (mm) t	Cutting Speed (m/min) V	Tangential Cutting Force(N) F_t	Feed Cutting Force(N) F_f
Test 1	10	0,02	0,03	3	115	70
Test 2	10	0,02	0,05	3	175	80
Test 3	10	0,02	0,1	3	310	105
Test 4	10	0,02	0,125	3	380	130
Test 5	5	0,005	0,01	6	46	35
Test 6	5	0,005	0,03	6	128	54
Test 7	5	0,005	0,05	6	175	65
Test 8	5	0,005	0,1	6	305	88
Test 9	10	0,005	0,01	6	44	27
Test 10	10	0,005	0,03	6	120	51
Test 11	10	0,005	0,05	6	169	56
Test 12	10	0,005	0,1	6	295	66
Test 13	10	0,01	0,01	6	125	65
Test 14	10	0,01	0,03	6	180	75
Test 15	10	0,01	0,05	6	235	90
Test 16	10	0,01	0,1	6	330	110
Test 17	10	0,02	0,03	6	130	80
Test 18	10	0,02	0,05	6	190	110
Test 19	10	0,02	0,1	6	345	130
Test 20	10	0,02	0,125	6	415	158
Test 21	15	0,005	0,01	6	41	25
Test 22	15	0,005	0,03	6	110	40
Test 23	15	0,005	0,05	6	165	46
Test 24	15	0,005	0,1	6	283	50
Test 25	10	0,02	0,05	12	210	130
Test 26	10	0,02	0,1	12	375	190
Test 27	10	0,02	0,125	12	462	220
Test 28	10	0,02	0,05	20	230	150
Test 29	10	0,02	0,1	20	412	221
Test 30	10	0,02	0,125	20	500	250

Table 2-5: FEA Tests Tangential and Feed Force Results.

Rake Angle (°)	Cutting Edge Radius (mm)	Cutting Speed (m/min)	K_{tc}	K_{te}	K_{fc}	K_{fe}
α_r	h_r	V	N/mm^2	N/mm	N/mm^2	N/mm
10	0,02	3	2769,2	33,9	605	50
10	0,02	6	3020,6	39,7	728,5	63,9
10	0,02	12	3351,4	41,8	1200	70
10	0,02	20	3605,7	50,2	1345,7	83,6
10	0,005	6	2717,3	27,9	379,9	31,9
10	0,01	6	2925,2	34,7	654,2	44,1
5	0,005	6	2790,8	30,9	558,4	33,8
15	0,005	6	2638,5	24,5	250,6	28,2

Table 2-6: Cutting Coefficients obtained from Advantedge Tests.

The cutting coefficients in each group is calculated and fitted to an equation according to the parameters.

$$\begin{aligned} K_{tc} &= 2522 - 15.2\alpha + 17103h_r + 47.2V \\ K_{fc} &= 377 - 30.8\alpha + 24479h_r + 44.9V \\ K_{te} &= 26.6 - 0.649\alpha + 638h_r + 0.851V \\ K_{fe} &= 17.8 - 0.563\alpha + 1840h_r + 1.78V \end{aligned} \tag{2.8}$$

where α in degrees, h_r in mm, V in m/min

Example 2-2

For the conditions expressed in Example 2-1 and taking h_r=0.010 mm and V=3.3528 m/min

$$K_{tc} = 2522 - 15.2\alpha + 17103h_r + 47.2V = 2669 \text{ N/mm}^2$$
$$K_{fc} = 377 - 30.8\alpha + 24479h_r + 44.9V = 363 \text{ N/mm}^2$$
$$K_{te} = 26.6 - 0.649\alpha + 638h_r + 0.851V = 28 \text{ N/mm}$$
$$K_{fe} = 17.8 - 0.563\alpha + 1840h_r + 1.78V = 35 \text{ N/mm}$$

	Tangential Cutting Force(N) F_t	Fitted Tangential Cutting Force(N) F_t	Feed Cutting Force(N) F_f	Fitted Feed Cutting Force(N) F_f
Test 1	115	121	70	74
Test 2	175	178	80	87
Test 3	310	321	105	120
Test 4	380	392	130	136
Test 5	46	60	35	41
Test 6	128	116	54	52
Test 7	175	172	65	64
Test 8	305	313	88	92
Test 9	44	56	27	36
Test 10	120	111	51	45
Test 11	169	165	56	53
Test 12	295	302	66	74
Test 13	125	116	65	58
Test 14	180	173	75	68
Test 15	235	314	90	96
Test 16	330	385	110	109
Test 17	130	128	80	83
Test 18	190	188	110	99
Test 19	345	338	130	138
Test 20	415	412	158	158
Test 21	41	52	25	32
Test 22	110	105	40	37
Test 23	165	158	46	43
Test 24	283	291	50	56
Test 25	210	207	130	123
Test 26	375	371	190	176
Test 27	462	453	220	203
Test 28	230	233	150	155
Test 29	412	415	221	226
Test 30	500	507	250	262

Table 2-7: Comparison of AdvantEdge Results and Fitted Values.

Also the shear angles of some cases (Table 2-8) are measured and the changes according to the parameters are investigated.

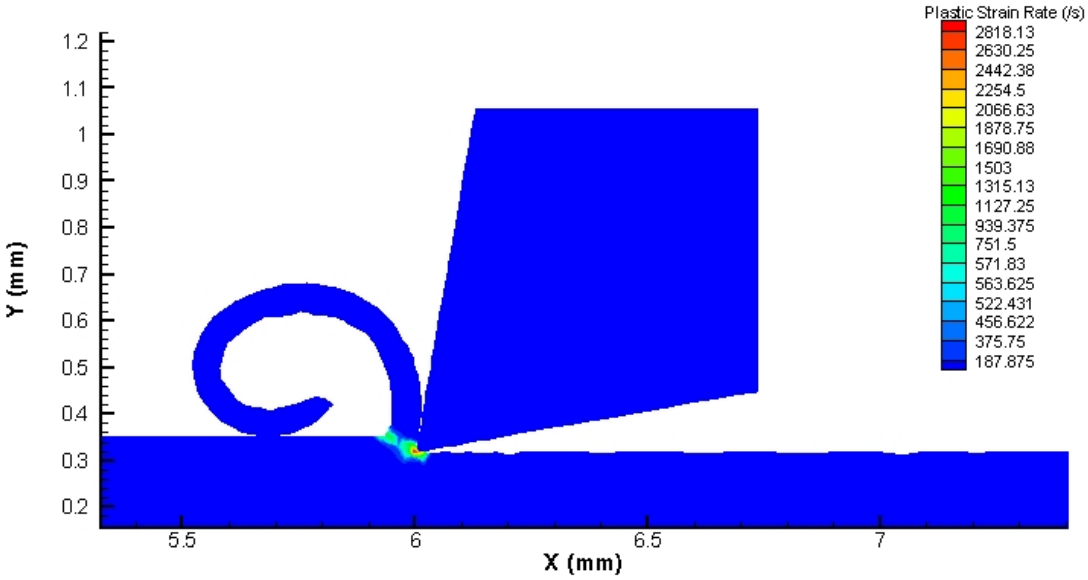

Figure 2-18: The plastic strain rate result of an Advantage test.

The zone where the plastic strain rate is maximum (as shown on Figure 2-18) is taken as shear plane and the angle of this zone with the horizontal is measured as shear angle.

	Rake Angle (°) α_r	Cutting Edge Radius (mm) h_r	Chip Load/tooth (mm) t	Cutting Speed (m/min) V	Shear Angle (°) ϕ_c
Test 1	5	0,005	0,03	6	23,3
Test 2	10	0,005	0,01	6	23,6
Test 3	10	0,005	0,05	6	27,7
Test 4	10	0,005	0,1	6	28,1
Test 5	10	0,02	0,05	6	26,5
Test 6	10	0,02	0,1	6	27,8
Test 7	10	0,02	0,125	6	28,9
Test 8	15	0,005	0,05	6	32,4
Test 9	15	0,005	0,1	6	34,2
Test 10	10	0,02	0,05	12	23,2
Test 11	10	0,02	0,1	12	24,4
Test 12	10	0,02	0,125	12	25,5
Test 13	10	0,02	0,05	20	22,3
Test 14	10	0,02	0,1	20	24,0
Test 15	10	0,02	0,125	20	24,3

Table 2-8: Shear Angle Test Matrix.

The effect of the parameters to the shear angle is seen on Table 2-8. As the rake angle increases, the shear angle also increases as expected. Also the chip load increases the shear angle. The tool wear has an inverse effect than the others. As the tip radius increases, it is observed that the shear angle decreases.

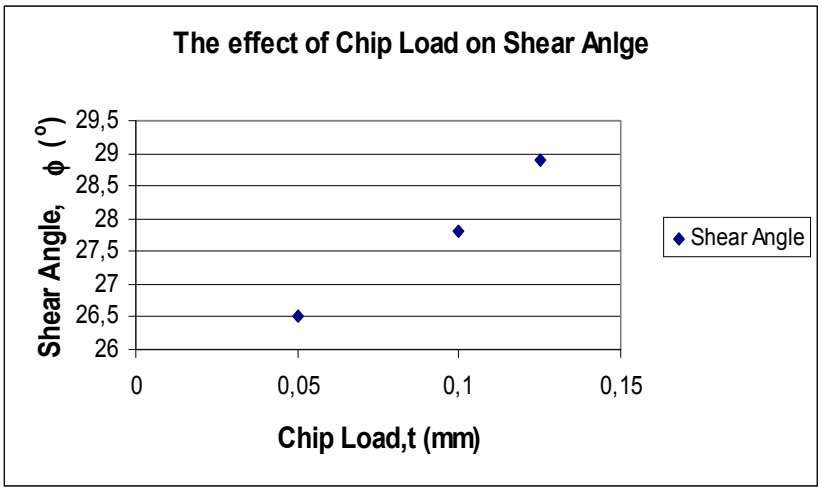

Figure 2-19: Chip Load effect on Shear Angle.

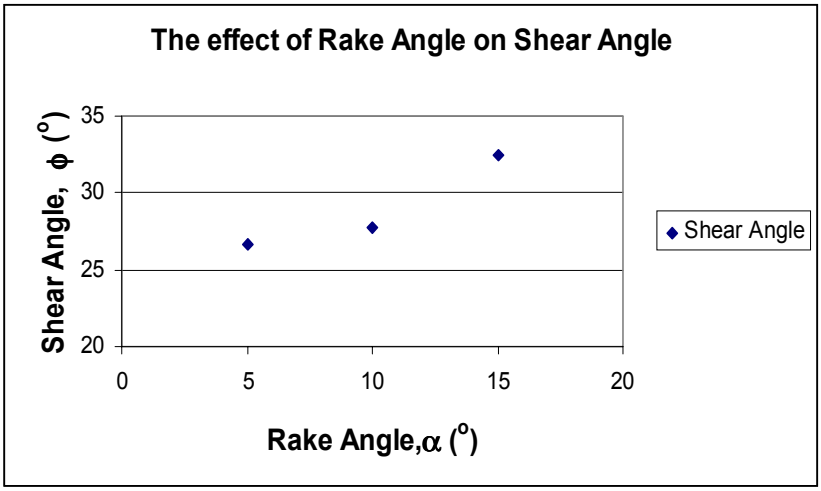

Figure 2-20: Rake Angle Effect on Shear Angle.

The shear angles are fitted to an equation regarding to the effects of chip load, cutting edge radius, rake angle, and cutting speed.

$$\phi = 21 + 0.711\alpha + 49.3t - 0.289V - 187h_r \quad (2.9)$$

A semi analytical FEA force model can be extracted by using the equation in Equation (2.2).

2.1.3 Experimental Force Model

Another method to obtain a force model is to carry out several cutting tests with different cutting conditions as in FEA force model. In this method, the cutting forces in tangential and feed dimensions are measured by using a force dynamometer. The dynamometer consists of four sensors containing three pairs of quartz plates, one sensitive to pressure in z direction and other two responding to shear in the x and y directions respectively. The dynamometer, three-component force measuring system, uses charge amplifiers, which convert the dynamometer charge signals into output voltages proportional to the force sustained.

It can be said that the experimental force model is more realistic and reliable because it is obtained from real cutting test. But sometimes it may not be possible to perform cutting tests because it can be expensive and time consuming.

Some cutting tests are performed by using real cutting conditions of broaching. HSS-T cutting tools are used to cut Waspaloy material. The other cutting conditions such as depth of cut, cutting speed and rake angle are chosen very near to broaching conditions.

The cutting coefficients are obtained as in Table 2-9 for different cutting speeds.

Cutting Speed [m/min]	3.3528	3.3528	3.3528	3.3528	3.3528	3.3528
Rake Angle [Deg]	4	6	8	10	12	14
Ktc [N/mm^2]	6189.93	5454.23	5506.79	5010.12	5387.30	4678.96
Kfc [N/mm^2]	3406.86	3275.01	3310.78	3242.31	3036.36	2345.22
Kte [N/mm]	79.59	87.42	79.43	77.93	61.00	75.69
Kfe [N/mm]	113.11	101.82	88.43	73.88	69.74	85.94
Average chip ratio, r_c	0.24	0.24	0.26	0.29	0.30	0.35
Average Shear Angle, ϕ_c [Deg]	13.41	13.50	14.88	16.54	17.54	20.25
Average Friction Angle, β_a [Deg]	31.30	36.11	37.18	41.59	40.68	40.27
Average Shear Strees, τ_s [MPa]	1200.21	1044.24	1132.20	1074.23	1255.14	1227.80

Table 2-9: Cutting Force Coefficient Data from real cutting tests.

Also the shear angle is obtained as

$$\phi = 9.3964 + 38.221t + 0.6267\alpha \tag{2.10}$$

2.1.4 Comparison of Models

When the three models obtained in Section 2.1.1 -2.1.3 are compared the following results are obtained.

For the same cutting conditions;

V=3.3528, b=1 mm, t=0.05 mm

The cutting forces are obtained by using equations (2.2), (2.8) and the results in Table 2-9 as follows

	Ft (N)	Ff (N)
Analytical Method	188.9	80.2
FEA Method	161.0	54.0
Experimental Method	330.4	221.6

Table 2-10: The comparison of the cutting forces obtained by three models.

	Ktc	Kte	Kfc	Kfe
FEA Method	2669.0	28.0	362	35
Experimental Method	5387.3	61.0	3036	69.74

Table 2-11: The comparison of FEA and Experimental Model.

It is seen that there is too much difference with the FEA model and the experimental model. So the FEA model is not reliable. The difference can arise from material models and flow models used in the software. The accuracy of the experimental model will be shown in section 4.1 with comparison to the real power data obtained from [30] together with the simulations results using the experimental model (Figure 4-4)

2.1.5 Calculation of total cutting forces using each model

The broaching forces on one tooth in both directions can be determined by multiplying the cutting force coefficients with the total chip area:

$$\begin{aligned} F_t &= K_t t_i b_i & F_t &= K_{tc} t_i b_i + K_{te} b_i \\ F_f &= K_f t_i b_i \quad \text{or} & F_f &= K_f t_i b_i + K_{fe} b_i \\ F &= \sqrt{F_t^2 + F_f{}^2} & F &= \sqrt{F_t^2 + F_f{}^2} \end{aligned} \tag{2.11}$$

So the total forces can be determined by multiplying the forces for one tooth by the number of teeth in cut;

$$\begin{aligned} F_t &= K_t \sum_{i=1}^{m} t_i b_i & F_t &= \sum_{i=1}^{m} \left(K_{tc} t_i b_i + K_{te} b_i \right) \\ F_f &= K_f \sum_{i=1}^{m} t_i b_i \quad \text{or} & F_f &= \sum_{i=1}^{m} \left(K_f t_i b_i + K_{fe} b_i \right) \end{aligned} \tag{2.12}$$

where m is the total number of teeth in cut, t_i and b_i are uncut chip thickness and width of cut for the tooth i. m depends on the cutter pitch and the part thickness whereas width of cut is determined by the periphery of the tooth which is in cut. It can be calculated as:

$$m = ceil(\frac{w}{p}) \tag{2.13}$$

where w is the part thickness and p is the pitch. The result of the division must be rounded to the nearest upper integer because m has to be an integer.

Example 2-3:

If the part thickness is 21 mm and pitch is 9 mm, then the number of teeth in cut can be calculated as:

$$m = ceil(\frac{thickness\ of\ the\ part}{pitch}) = ceil(\frac{21}{9}) = 3$$

2.2 Power Model

As broaching is a slow cutting process one may think the power will be low. However, but due to multiple teeth cutting at the same time, the power consumed by a broaching machine reaches to high levels. As the number of teeth in cut increases, the power required by the process increases as well.

Due to the fact that higher power requirements are needed, the power consumed has to be calculated and the necessary modifications have to be done at the design stage.

The total power drawn can be calculated as:

$$P = F_t.V = \sum_{i=1}^{m} t_i b_i K_t.V \text{ or } P = F_t.V = \left(\sum_{i=1}^{m} t_i b_i K_{tc} + \sum_{i=1}^{m} b_i K_{te} \right).V \tag{2.14}$$

Substituting equation (2.13) into equation (2.14) and assuming that the chip thickness and the width of cut are the same on the simultaneously cutting teeth, the following is obtained:

$$P = \frac{wtbK_tV}{p} \tag{2.15}$$

Equation (2.15) can be used to determine limitations on *t, V* and *p* due to power constraint as expressed in the following

$$\begin{aligned} t &\le \frac{Pp}{bwK_tV} \\ V &\le \frac{Pp}{btwK_t} \\ p &\le \frac{btwK_tV}{P} \end{aligned} \tag{2.16}$$

For a simple case where there is only one broach section, the formulation can be simplified as follows. If the total stock which needs to be removed from the surface *is s*, for constant rise per tooth (*t*), the necessary number of teeth on the cutter is

$$N = s / t \tag{2.17}$$

The total length of the broach is

$$L = N.p = \frac{s}{t} p \tag{2.18}$$

From which the chip thickness in terms of other parameters is obtained as

$$t = \frac{sp}{L} \tag{2.19}$$

Substituting equation (2.19) into equation (2.15):

$$P = \frac{bwsK_t V}{L} \tag{2.20}$$

Similar to equation (2.16), the limitations on the maximum stock size and velocity can be determined in terms of the broaching system parameters:

$$\begin{aligned} s &\leq \frac{LP}{bwK_t V} \\ V &\leq \frac{LP}{bwsK_t} \end{aligned} \tag{2.21}$$

2.3 Chatter Stability Model

Chatter vibrations may develop and result in poor surface finish in broaching. It could be an important limitation particularly for highly flexible parts and fixtures. Broaching is an orthogonal cutting process, and thus standard cutting stability model can be used for determining the limiting width of cut which dictates the allowable number of teeth in cut. The chatter stability limit for the width of cut in orthogonal cutting is given by [39].

$$b_{\lim} = -\frac{1}{2\,\mathrm{Re}[G]K_f} \tag{2.22}$$

where G is the oriented transfer function in the chip thickness direction. In broaching, the total width of cut must be smaller than the stability limit:

$$\sum_{i=1}^{m} b_i \le b_{\lim} \tag{2.23}$$

The width of cut is usually the same for successive broaching teeth:

$$b_i \le \frac{b_{\lim}}{m} \quad or \quad m \le \frac{b_{\lim}}{b_i} \qquad i=1,..,\ n \tag{2.24}$$

2.4 Summary

In this chapter, process models for broaching are presented. First of all, force models are developed using three different approaches. The experimental model is the most accurate one because it is based on the real cutting tests. The analytical model results are different than the experimental model results. The FEA model results are considerably different. For this reason FEA results are not reliable. But the trends of the forces with cutting conditions such as chip load, cutting speed, rake angle and tool tip radius are helpful in the analysis. It can be proposed that the FEA may not be an accurate modeling tool for machining processes due to several reasons. First of all, the material data for extreme conditions of machining are not available. Also, tool-workpiece friction is difficult to predict accurately. Power model is also based on the force model. Finally the stability model is checked in order to prevent chatter.

CHAPTER 3 STRUCTURAL MODELING

Constraints due to structural deformations and stresses are important part of broaching process modeling and optimization. In this chapter, models developed for tooth stress and part deformations will be presented.

Many tooth geometries can be obtained by varying the parameters shown in Figure 3-1. It will later be shown that even complex tooth profiles can be represented by this model for stress analysis.

3.1 Tooth Stress

Broaching forces can be quite high due to large width of cuts which may be required by a given profile. High forces may cause tooth breakage, thus tooth stresses must be considered during tool design. Tooth stress analysis can be performed using the Finite Element Analysis (FEA). Broach tooth profiles can have variety of complex shapes which makes the stress analysis time consuming as analysis of each profile needs to be performed separately. In order to simplify and generalize the modeling, generalized tooth geometry has been used in FEA as shown in Figure 3-1.

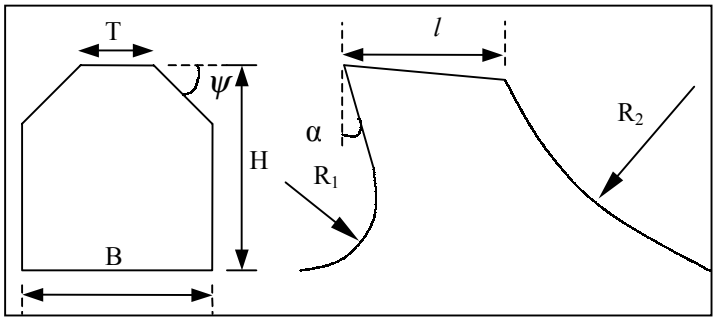

Figure 3-1: Generalized broach tooth profile used in the stress analysis.

Test No.	H (mm)	B (mm)	T (mm)	ψ (^{o})	R_1 (mm)	l (mm)
1	4	4	2.8	15	2	4
2	4	4	2.8	15	2	4.5
3	4	4	2.8	15	2	5
4	4	2	1.5	25	1	4
5	4	2	1.5	25	1.5	4
6	4	2	1.5	25	2	4
7	4	2	1.5	25	2.5	4
8	4	4	2	15	2	4
9	4	4	2	25	2	4
10	4	4	2	35	2	4
11	4	4	2.8	15	2	4
12	3	4	2.8	15	2	4
13	5	4	2.8	15	2	4
14	6	4	2.8	15	2	4
15	3	1.3	1	45	2	4
16	3	2.5	1	45	2	4
17	3	3.5	1	45	2	4

Table 3-1: Tooth Stress FEA Test Matrix.

A test matrix is formed in order to determine the effect of each parameter on the tooth stress. In the third direction, a standard clearance angle of 2^o is used for fir-tree broaches which is commonly used on broach tools. FEA is used for stress analysis of each case. The results of these analyses are used to develop a generalized equation for stress prediction in broach teeth.

Young's Modulus	2.068E+011 N/m^2
Poisson Ratio	0.26
Density	8600 kg/m^3
Yield Strength	6.278E+008N/m^2

Table 3-2: HSS-T material properties.

HSS-T material (Table 3-2) is used in the FEA in Catia v5r8. Tetrahedron element type is used. Critical sections such as force application points and gullet surfaces are meshed finer with an element size of 0.2 mm, the others are meshed coarser with element size of 0.5 mm. The cutting forces in tangential and feed direction were

distributed at the cutting edges of the tooth in a uniform manner. The maximum stresses in the tooth body were determined using the FEA as shown in Figure 3-2.

The maximum stresses occur at the vicinity of the forced application point and at the gullet surface. The stresses at the gullet surface are read and recorded in Table 3-3.

Test No.	FEA Stresses (MPa)	Stress Values by using Eqn 3.1 (MPa)	Error (%)
1	190	187	2
2	175	179	2
3	173	173	0
4	205	214	4
5	176	207	18
6	185	202	9
7	176	198	13
8	183	184	0
9	190	198	4
10	201	215	7
11	190	187	2
12	174	168	4
13	200	203	2
14	246	217	12
15	234	206	12
16	227	220	3
17	223	222	1

Table 3-3: FEA Stress Results and Comparison with fitted values.

Then the following equation has been determined by curve-fitting for the maximum stress in the tooth as a function of different tooth geometry parameters:

$$\sigma_t = F(1.3H^{0.374}B^{-1.09}T^{0.072}\psi^{0.088}R_1^{-0.082}l^{-0.356}) \qquad (3.1)$$

where dimensions are in (mm), ψ is in degrees and σ is in (MPa). F is the total cutting force on one tooth obtained by Equation (2.11). The general form shown in Figure 3-1 is also a valid representation for more complex tooth-forms such as a fir-tree. This was checked by comparing results from FEA and equation (3.1).

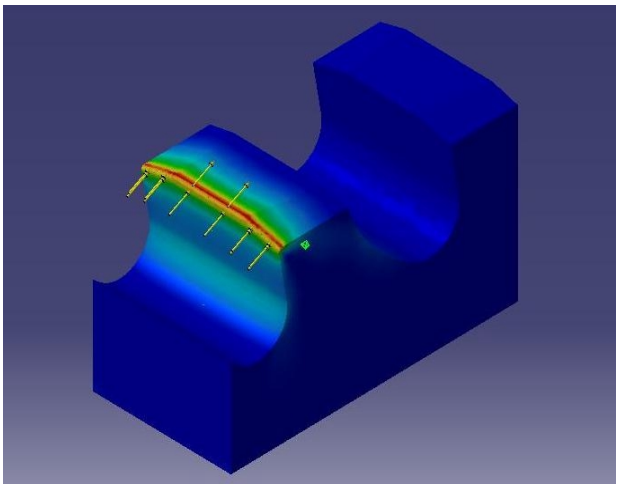

Figure 3-2: Broach tooth stress predictions using FEA.

3.2 Part Quality

Form errors left on a machined surface are considered as one of the measures of the part quality. They increase with cutting loads resulting from high rise per tooth, high number of teeth in cut or worn cutting teeth. The force and part deflection models can be used in order to predict form errors in broaching. For a specified maximum allowable form error, the chip load or number of teeth in cut may be modified to achieve the desired quality. This can be expressed as follows.

$$F_q / k_q = \delta_q$$
$$or \qquad (q=t,f) \qquad (3.2)$$
$$\frac{K_q t}{k_q} \sum_{i=1}^{m} b_i \le \delta_{allowed}$$

where k_q, K_q, δ_q are the stiffness, cutting force coefficient and deflection in the direction of interest, i.e. tangential (t) or feed (or passive) (f) directions, respectively. b_i is the width of cut for tooth i, $\delta_{allowed}$ in the maximum deflection allowed which is dictated by part tolerances.

During broaching process, cutting teeth enter and leave the part continuously and the number of teeth in cut changes. The cutting forces are directly proportional to the number of teeth in cut. As the forces increase, the deflection of the part increases. Furthermore, cutting teeth moves continuously which results in variation of force application location.

Deflection models developed for a generalized part geometry will be presented in the following sections.

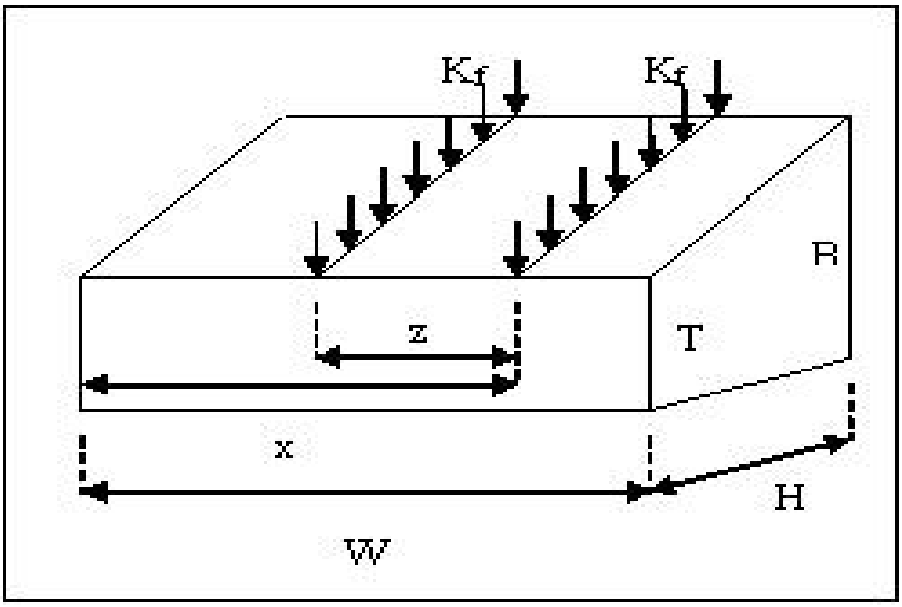

Figure 3-3: Generalized part geometry used in the deflection analysis.

3.2.1 Energy Method

In this section, energy method is used to find the deflection in generalized part geometry analytically.

Strain energy can be defined as the energy associated with the deformation of the member. The strain energy is equal to the work done by a slowly increasing load applied to member. The strain energy density of a material –the strain energy per volume- is equal to the area under the stress-strain curve of the material.

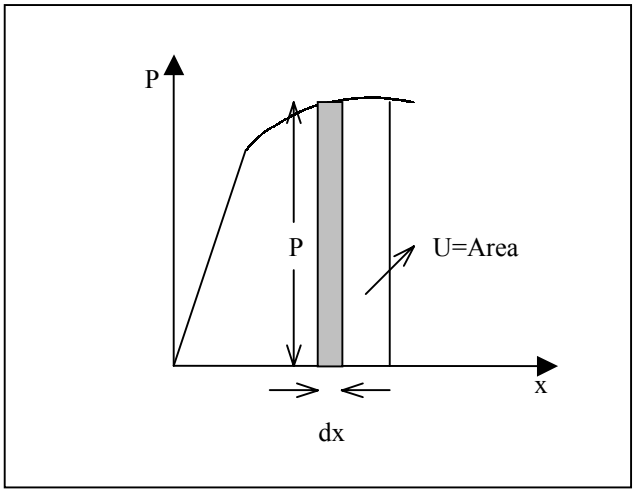

Figure 3-4: Load deformation diagram.

The strain energy

$$dU = Pdx$$

$$Strain\ energy = U = \int_0^{x_1} Pdx \tag{3.3}$$

The strain-energy density

$$Strain\ energy = u = \int_0^{\varepsilon_1} \sigma_x d\varepsilon_1 = \frac{dU}{dV} \tag{3.4}$$

Substitute equation (3.3) in equation (3.4)

$$U = \int \frac{\sigma_x^{\ 2}}{2E} dV \tag{3.5}$$

Since the fir-tree profile is a very complex shape, it has to be simplified to a basic shape.

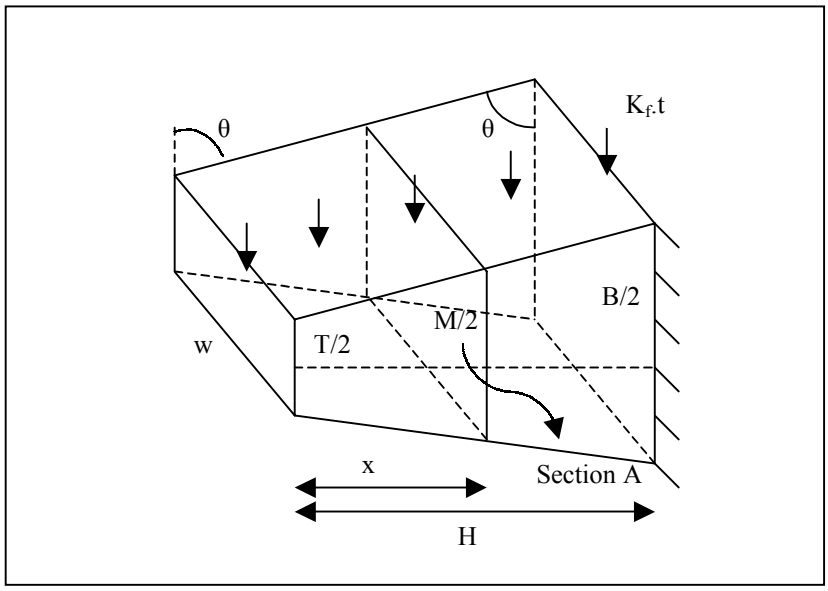

Figure 3-5: Timoshenko Beam.

The part geometry is represented by the generalized shape shown in Figure 3-5. Similar to the tooth geometry, this shape is very convenient as it can represent many different part geometries by varying the parameters *H*, *T*, *W*, and *B*. It will be shown later that this form can be used to approximate very complex geometries such as a fir-tree accurately. It can be modeled as Timoshenko beam [41] and the maximum deflection of the beam can be calculated by Energy Method.

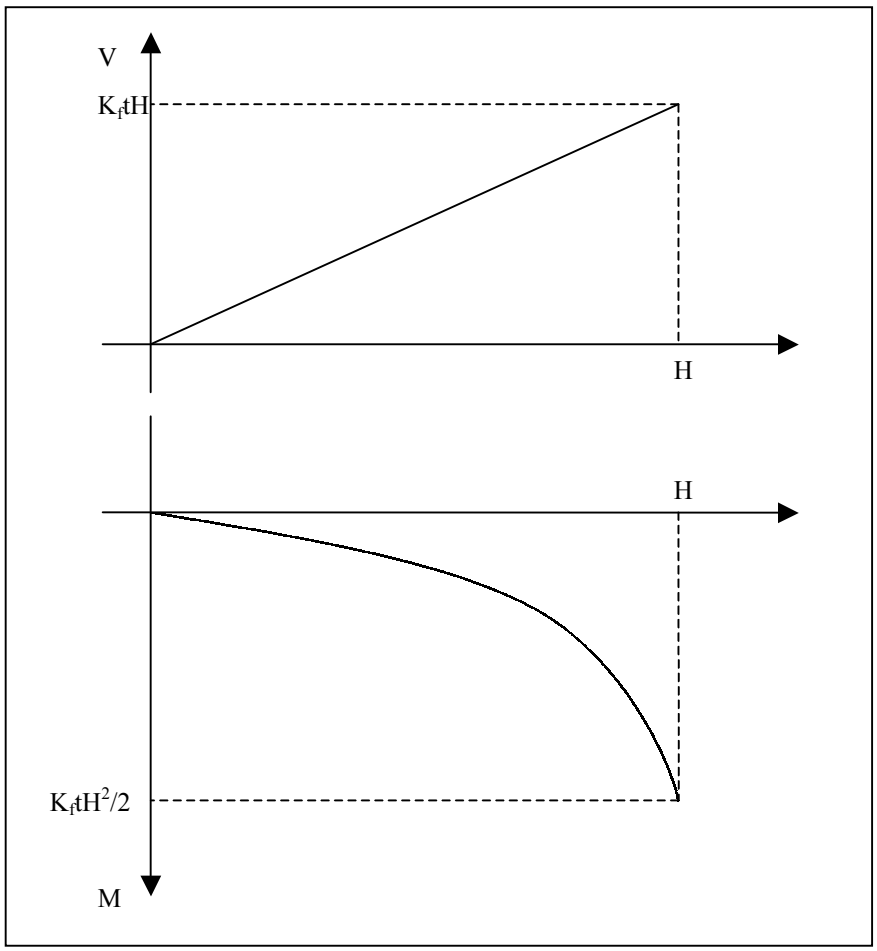

Figure 3-6: Shear and Moment diagrams of Timoshenko beam.

The total strain energy can be expressed as;

U = Strain energy in bending + Strain energy in shearing

$$U = \int_0^H \frac{M^2}{2EI} dx + \int_0^H \frac{\tau_{xy}^{\ 2}}{2G} dV \tag{3.6}$$

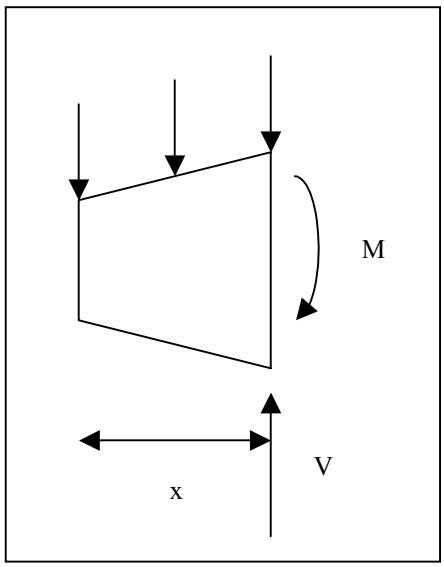

Figure 3-7: Free body diagram of Timoshenko beam.

The bending moment and shear force shown in Figure 3-7 can be expressed as follows;

$$M(x) = \frac{K_f t x^2}{2} \;\&\; V(x) = K_f t x \tag{3.7}$$

The moment of inertia along the x-direction can be determined as;

$$I(x) = \frac{1}{12} w(y)^3 \quad \text{where} \quad y = 2(T/2 + \frac{x}{\tan(\theta)})$$

$$I(x) = \frac{1}{12} w(T + \frac{2x}{\tan(\theta)})^3 \tag{3.8}$$

The shear stress can be calculated as

$$\tau_{xy}(x) = \frac{V(x)Q(x)}{I(x)w} \tag{3.9}$$

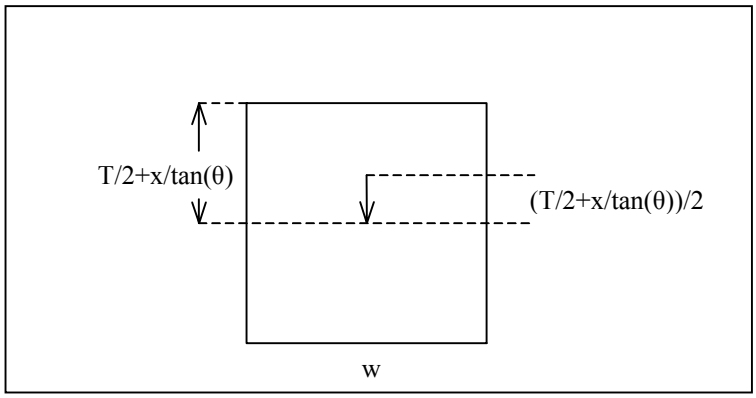

Figure 3-8: Cross-section of the Timoshenko beam.

$$Q = (\frac{T}{2} + \frac{x}{\tan\theta})w\frac{(\frac{T}{2} + \frac{x}{\tan\theta})}{2} \tag{3.10}$$

$$\tau_{xy} = \frac{K_f tx(\frac{T}{2} + \frac{x}{\tan\theta})w\frac{(\frac{T}{2} + \frac{x}{\tan\theta})}{2}}{\frac{1}{12}w(T + \frac{2x}{\tan(\theta)})^3 w} \tag{3.11}$$

$$dV = (T + \frac{2x}{\tan\theta})dx \tag{3.12}$$

Equations from (3.7) to (3.12) can be substituted in to (3.6) to determine the total strain energy as follows;

$$U = \int_0^H \frac{\left(\frac{K_f tx^2}{2}\right)^2}{2E\frac{1}{12}w(T + \frac{2x}{\tan(\theta)})^3}dx + \int_0^H \frac{\left(\frac{K_f tx(\frac{T}{2} + \frac{x}{\tan\theta})w\frac{(\frac{T}{2} + \frac{x}{\tan\theta})}{2}}{\frac{1}{12}w(T + \frac{2x}{\tan(\theta)})^3 w}\right)^2}{2G}(T + \frac{2x}{\tan\theta})dx \tag{3.13}$$

The strain energy must be equal to the total work done by the external force.

$$Strain\ Energy = U = \int_0^{y_1} Fdy$$

where F is the total cutting force and the y_1 is the deformation under loading

$$U = \int_0^{y_1} Fdy = \int_0^{y_1} K_f tHdy \tag{3.14}$$

$$U = \frac{1}{2}K_f tHy_1$$

From which the deflection can be determined as

$$y_1 = \frac{2U}{K_f tH} \tag{3.15}$$

But there is a missing point in energy method because the application point is not considered in this model.

In this model when there are two or more than two teeth in cut, the deflection can simply be calculated by multiplying y_1 by the number of teeth in cut. Thus

$$y = my_1 \tag{3.16}$$

where m is the number of teeth in cut.

3.2.2 FEA Method

By using FEA method, more accurate modeling of the part geometry can be achieved and the force application points can also be considered. Since fir-tree is one of the most complex broached geometry, it is approximated according to the analyses below as in Energy method.

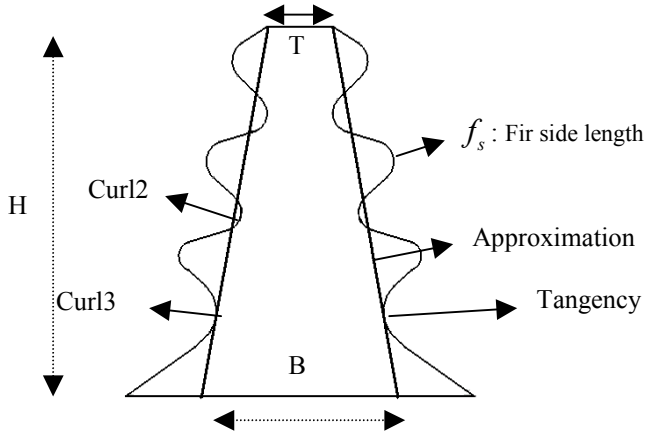

Figure 3-9: Fir-tree approximation.

The approximation shown in Figure 3-9 is used in the analysis. First, the accuracy of the trapezoidal approximation is checked using FEA which is given in Table 3-4. In this analysis, the same force is applied both to the 1st approximation and 2nd approximation. Then it is compared with the equation result obtained form (3.17). As it can be seen from the table, the approximation is quite acceptable and representing a fir-tree by drawing a tangent line to curl 3 is better than curl 2.

	Tangent to curl 2			Tangent to curl 3		
	FEA	Formula	Error	FEA	Formula	Error
Case 1	0.184	0.198	8%	0.165	0.160	3%
Case 2	0.184	0.196	7%	0.184	0.176	4%

Table 3-4: Fir-tree approximation comparison.

Therefore, the geometry shown in Figure 3-3 can be used as the generalized geometry. Similar to the tooth stress analysis, the geometric parameters have been varied in the FEA, and the following resulting equation has been determined through

curve-fitting for the prediction of deflection at a point ($x.w$) when the force, i.e. cutting tooth, is at the same position as shown in Figure 3-3:

$$\delta_{i,x}^{p} = \frac{K_f f_s t}{1000}(0.0265 w^{-0.45} T^{-0.608} B^{-1.834} H^{1.81} r_1^{0.968}) \tag{3.17}$$

$\delta_{i,x}^{p}$: deflection caused by tooth i at position x when it is at position x (mm)

r_1: ratio of the force application location to the width of the part

where $\left\{ \begin{array}{l} r_1 = 1 - \frac{x}{w} \text{ if } r_1 < 0.5 \\ r_1 = \frac{x}{w} \quad \text{if } r_1 \geq 0.5 \end{array} \right\}$

The equation is fitted according to the ratios greater than 0.5 because of the symmetricity of the part. For example, the deflection at the r_1=0.7 is equal to the r_1=0.3. For this reason, 0.5 is added to the ratio for the ratios lower than 0.5 to obtain the accurate deflection value.

If multiple teeth are in cut at the same time, the deflection caused by one of the cutting tooth at the position where the other tooth is in contact with the material is approximated as:

$$\delta_{j,x}^{e} = \frac{K_f f_s t}{1000}(0.005 w^{-1.35} T^{-0.259} B^{-1.81} H^{2.47} r_2^{-1.16}) \tag{3.18}$$

$\delta_{j,x}^{e}$: deflection caused by tooth j at position x when it is at a distance z from x (mm) where $r_2 = \frac{z}{w}$. Using super positioning of deflections caused by all teeth, the deflection of the part during cutting is found. Note that fixture stiffness must be measured if it is significant. The total deflection at a point can be calculated as:

$$\delta_x = \delta_{i,x}^{p} + \sum_{j \neq i}^{m} \delta_{j,x}^{e} \qquad \text{(mm) } j = 1 : m \tag{3.19}$$

3.3 Summary

In this chapter, models are developed for tooth stress and part deformations which are very important for the improvement and the optimization of the broach tool design. These models will later be integrated into the simulation program and optimization program which will be discussed in Chapter 4 and Chapter 5.

CHAPTER 4 SIMULATION OF BROACHING PROCESS

In machining processes, prediction of the outputs such as cutting forces, tooth stresses, part quality are very important at the design stage and for the cutting parameter selection. Although there exist several commercial software for machining simulation, most of them are for milling and turning. The models developed in Chapter 2 and Chapter 3 will be used in simulations.

A computer program has been developed in Matlab in order to simulate the process and improve the tool design. The inputs to the program are the material characteristics, tool and part geometry. The predicted forces depending on the force model, power, tooth stresses and part deflections are outputs of the program. The simulation is carried out in time domain where the broach tool is advanced into the material using small increments. In every step the broach tool position is moved by one increment and checked whether it is inside the part –in cut- or not. Then the necessary calculations are done for each increment and the results are presented.

There are two modes in the program. In the simple mode, the effects of deflections on cutting force calculations are neglected (Rigid Model) whereas in the iterative mode, the deflection effects are included (Flexible Model).

4.1 Rigid Model

In rigid model, the effect of workpiece deflection on the forces is neglected. So the program is simpler and the computation time is shorter. The algorithm of the program is shown on the Figure 4-2.

Example 4-1:

An example simulation for specified tool geometry for fir-tree production is carried out by using cutting conditions as;

V=0.056 m/s

Rake angle=12

By using experimental force coefficients in Table 2-9;

K_t=5387 N/mm^2 K_{te}=61 N/mm

K_f=3036.36 N/mm^2 K_{fe}=69.74 N/mm

The force predictions are obtained as in Figure 4-1.

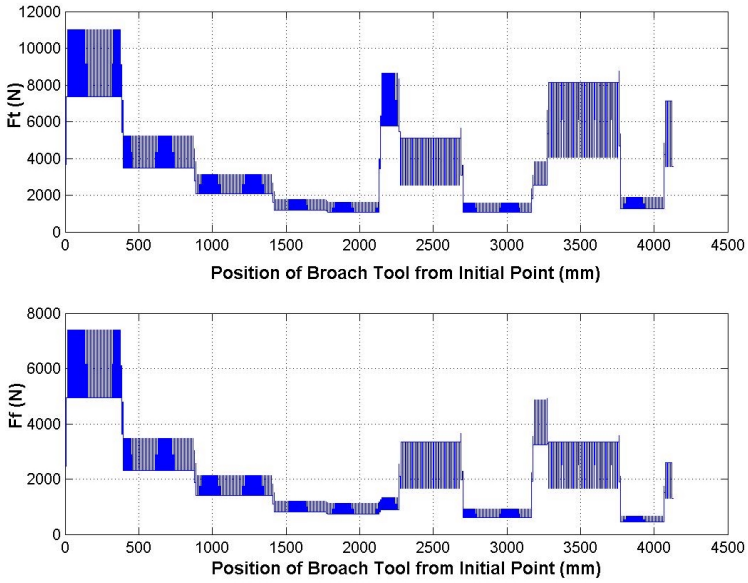

Figure 4-1: Tangential and Feed force prediction.

The forces are calculated for the teeth in-cut when the tool is moved by one increment. Then the forces at each step are combined and presented. The forces vary form section to section because of the change in cutting parameters. The forces also vary in a section because of the number of teeth in cut changes continually. In transitions between the sections the forces increases or decreases gradually.

In order to verify the force predictions, power monitoring data [30] shown on Figure 4-3 is used. The power of the process is calculated as stated in section 2.2 and compared with the monitoring data in Figure 4-4. The bold line in Figure 4-4 is the process power read from Figure 4-3. It is seen that the prediction results correlates with the monitoring data reasonably well.

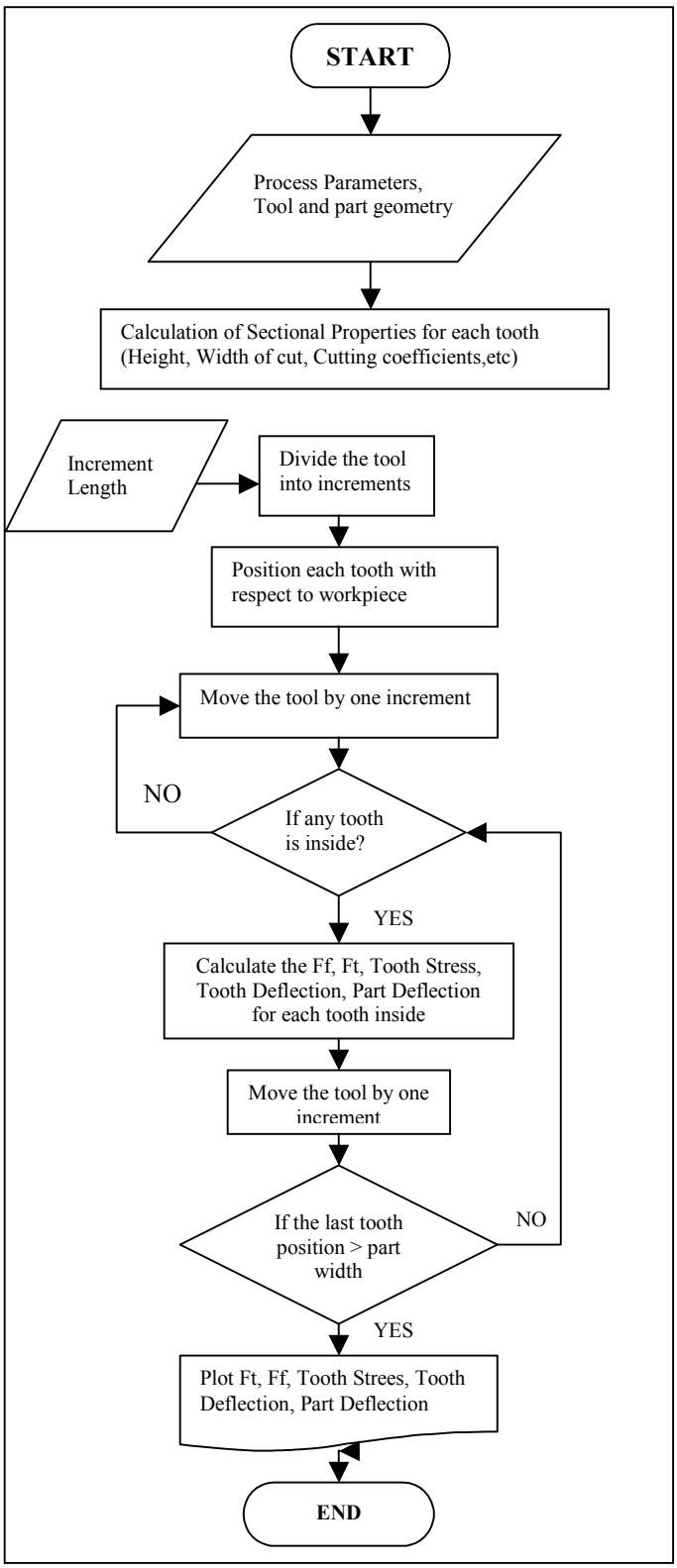

Figure 4-2: Algorithm of Rigid Model.

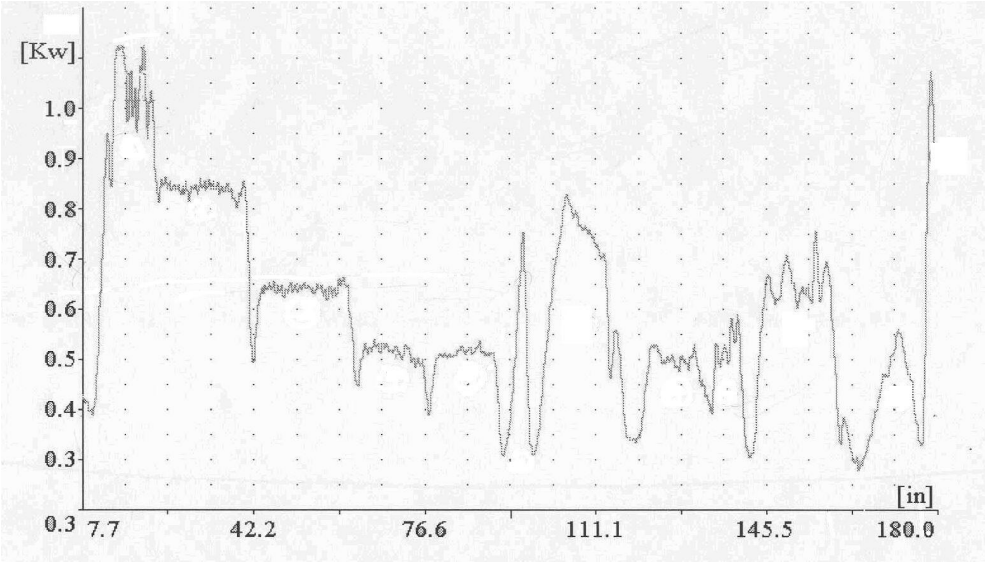

Figure 4-3: Power data from monitoring results [30].

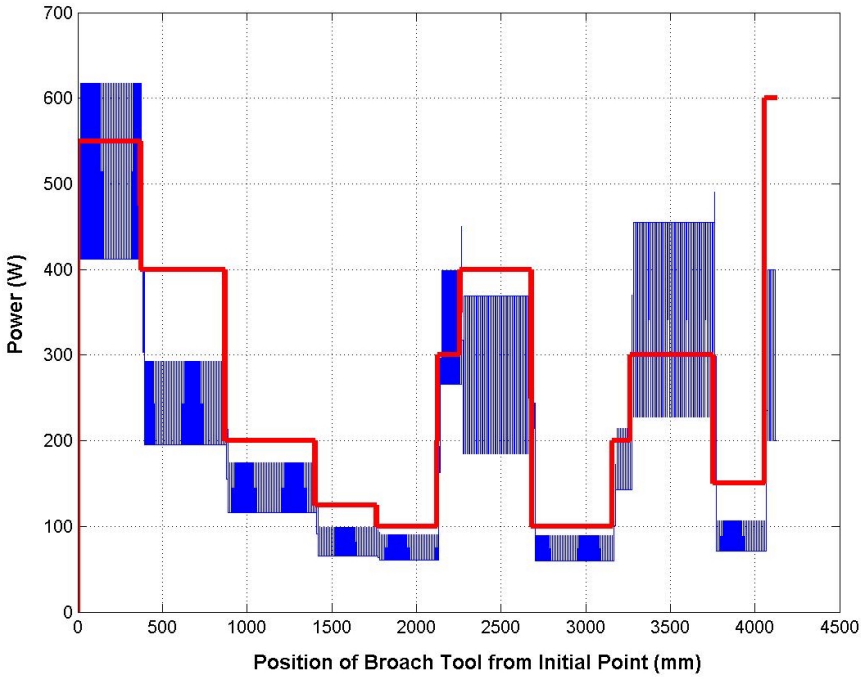

Figure 4-4: Power data comparison.

According to the tooth stress model obtained in section 3.1 , the stress predictions in each section is determined and shown in Figure 4-5. In some sections the stress values increase because of the rise per tooth. The values are below the permitted stress limit in order to prevent tooth breakage.

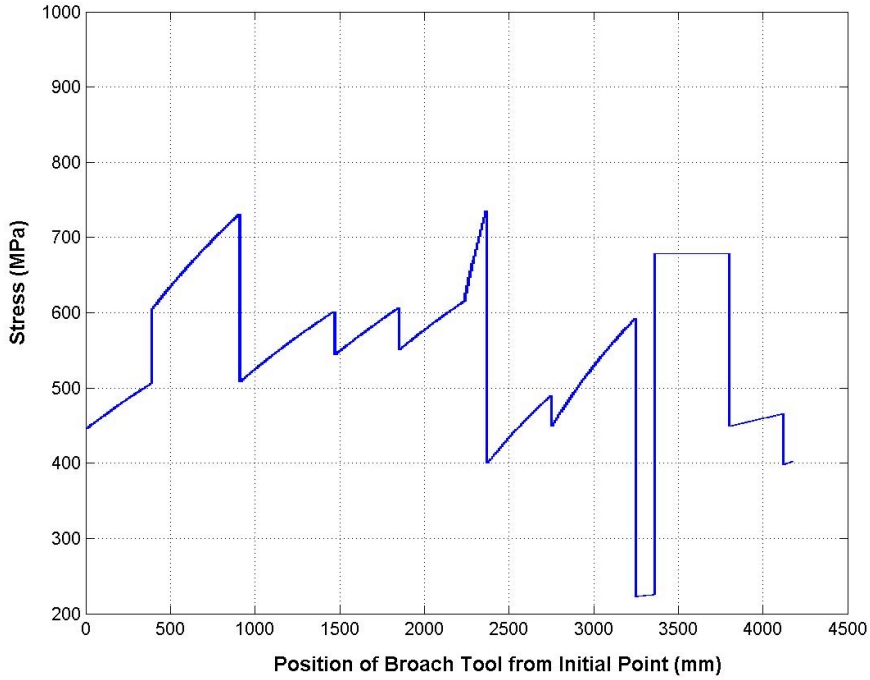

Figure 4-5: Stress Prediction.

The form errors on the surface can be predicted by the model developed in section 3.2.2. According to the model, there are some assumptions that must be mentioned. The form errors left on the surface by roughing and semi-finishing teeth are disregarded. Only the maximum deflection of the part during finishing is considered. From quality point of view, the maximum form error is the most important parameter.

The maximum form error is obtained as 29.2 μm.

4.2 Flexible Model

In the flexible model the effects of deflections are considered in force calculations. The cutting forces cause deflections on the part and results in less chip load than proposed. The deflection of the workpiece is calculated by using an average stiffness value for the part. A sample chip load variation for a process in which two teeth in cut at the same time caused by workpiece deflection is simulated and shown in Figure 4-6.

As shown on the figure when the first tooth starts to cut, the proposed chip load t_1 is decreased because of the workpiece deflection. In order to simplify the representation, the part deflections are represented by tooth deflections of the same amount which has exactly the same effect on the chip thickness and cutting force. When the second tooth starts to cut, the cutting force is doubled, and so does the workpiece deflection. The proposed chip load for the first tooth t_1 and second tooth t_2 decreases as well. When the first tooth exits the workpiece, the cutting force and workpiece deflection decreases. The same process occurs at the entrance and exit of the other teeth. The arrows in Figure 4-6 show that the tooth deflects up or down in the arrow direction. The process is simulated using the algorithm shown in Figure 4-9.

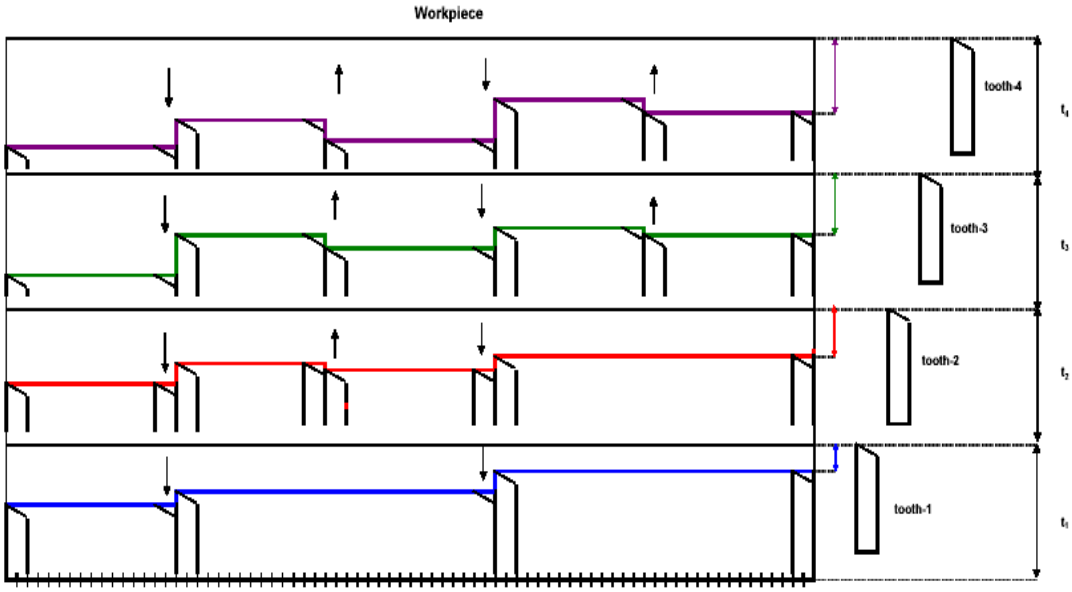

Figure 4-6: Simulation of workpiece deflection and chip load per tooth.

Example 4-2:

For a broaching process with cutting conditions;

V=0.056 m/s

Rake angle=12

Section #	**1**	**2**	**3**	**4**	**5**
chip load	0,0457	0,0508	0,0406	0,0356	0,0356
tooth width	4,3180	4,5812	1,7493	2,1082	1,9558

By using experimental force coefficients in Table 2-9;

$K_t=5387\ N/mm^2$ $K_{te}=61\ N/mm$

$K_f=3036.36\ N/mm^2$ $K_{fe}=69.74\ N/mm$

The resulting feed force is as shown in Figure 4-7. The enlarged views of some sections are shown in Figure 4-8. It is seen that the deflections affect the forces on the first few teeth after which they stabilize. Therefore, rigid model is used in the rest if the analysis as it is much more practical and fast.

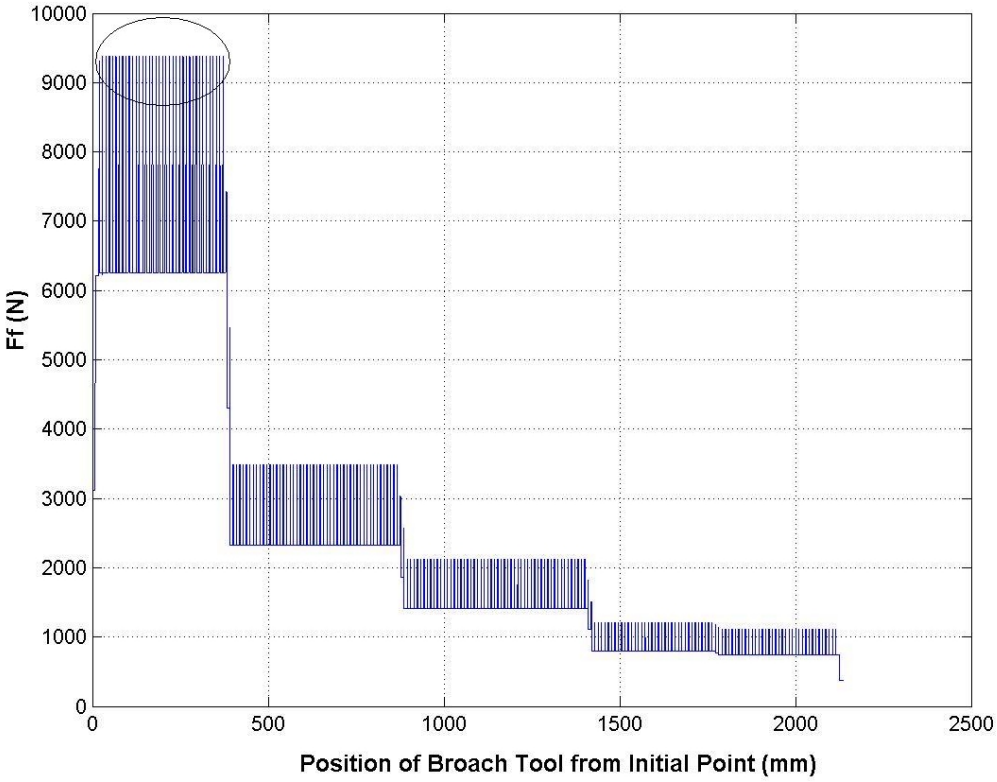

Figure 4-7: Feed force simulation.

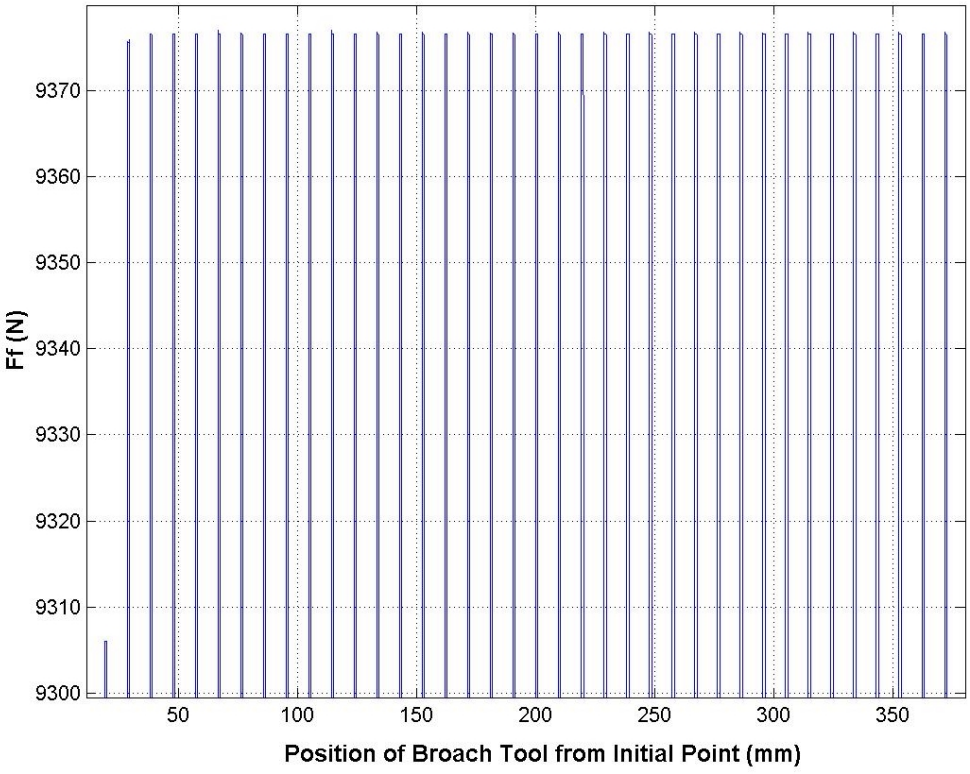

Figure 4-8: Enlarged view of the circled part in Figure 4-7.

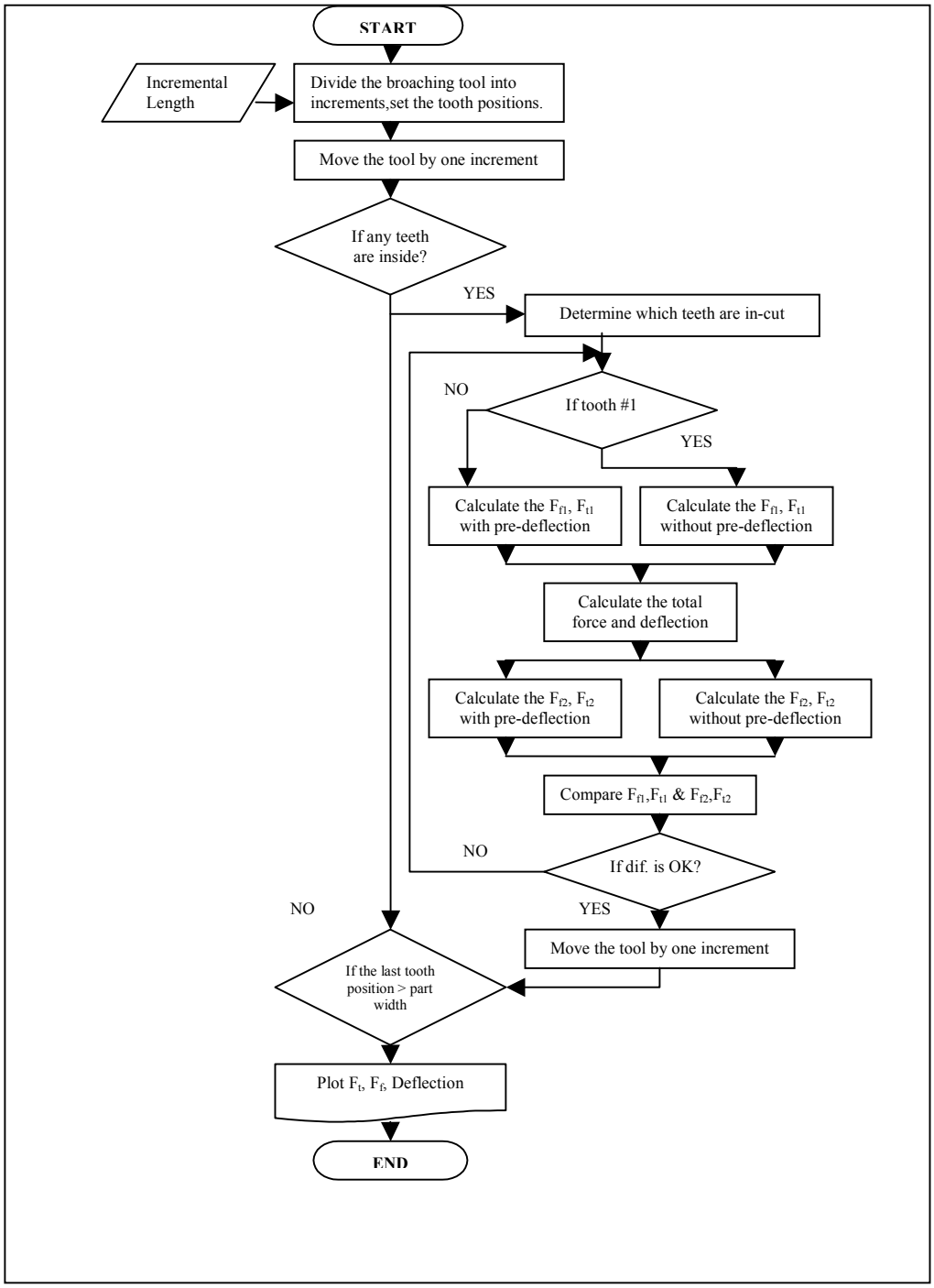

Figure 4-9: Algorithm of Flexible Model.

4.3 Summary

In this chapter, the models obtained in Chapter 2 and Chapter 3 are integrated into a simulation program coded in Matlab. The cutting force, power, tooth stress and part deflection predictions are obtained from the program. These predictions will be used in order to improve the broach tool design which is described in Chapter 5 in detail.

CHAPTER 5 IMPROVEMENT AND OPTIMIZATION IN TOOL DESIGN

The improvement of the process and tool design can be achieved through modeling. In order to achieve the desired productivity, predictive models are very important. As in other operations, higher productivity and lower cost are the objectives in broach optimization as well. For that reason, the most logical approach is to increase the material removal rate or reduce the cuttting time in a broach cycle. The simulations presented in the previous chapters indicate that there is opportunity for improvement on tool design. The tool design can be improved by applying the several methods presented in this chapter.

5.1 Improvement in Broach Tool Design

The first improvement is achieved by varying two main parameters -rise per tooth and pitch- for optimization. The main objective is to reduce the tool length by respecting all the constraints. The improvement is always started by varying the rise as it is a much simpler parameter to physically modify on the tools. After this is completed, the pitch is varied in each section in order to reduce the length further, by again respecting the constraints.

As a first step, the rises in all sections were increased or decreased until a constraint is encountered. The maximum or minimum chip thicknesses are usual limitations as well as tooth stress and part deflections. Next, the pitch was decreased in order to reduce the length, increase the force, and thus reduce the force fluctuation.

The force fluctuation with the original tool design is as high 430 % which was reduced significantly. Stresses on roughing teeth are kept below 850 MPa in order to prevent tooth breakage. Also the stresses on finishing teeth are lower compared to roughing teeth. Chip space may become an important limitation for small pitches which reduce the chip space significantly. The chip space to chip area ratio was found to be minimum of about 4. Considering the recommended 2-4 range in Monday [23], a minimum of 3 has been used in simulations.

	1		2		3		4		5		6	
	Before	**After**	**Before**	**After**	**Before**	**After**	**Before**	**After**	**Before**	**After**	**Before**	**After**
Number of teeth	39	31	52	47	56	45	38	30	38	30	14	14
Pitch (mm)	9.525	7.1	9.525	7.1	9.525	5.3	9.525	4.9	9.525	4.9	9.525	8.5
Section Length (mm)	371.5	221.5	495.3	335.6	533.4	237.4	362.0	148.9	362.0	148.9	133.4	119
Number of teeth in cut	3	3	3	3	3	4	3	5	3	5	3	3
Volume Ratio	5%	12%	6%	14%	5%	24%	4%	20%	4%	21%	27%	40%
	7		**8**		**9**		**10**		**11**		**12**	
	Before	**After**	**Before**	**After**	**Before**	**After**	**Before**	**After**	**Before**	**After**	**Before**	**After**
Number of teeth	38	33	50	50	11	11	44	73	32	32	6	6
Pitch	11.125	11.125	9.525	6	9.525	7.1	11.125	11.125	9.525	7.1	11.125	21.25
Section Length	422.8	367.6	476.3	300	104.8	78.1	489.5	815.8	304.8	227.2	66.8	127.5
Number of teeth in cut	2	2	3	4	3	3	2	2	3	3	2	1
Volume Ratio	18%	29%	6%	17%	1%	3%	7%	6%	2%	4%	6%	2%

Table 5-1: Modifications on broach tool design.

After the modifications listed in Table 5-1, the cutting force and tooth stress predictions are shown for the new geometry in Figure 5-1 and Figure 5-2, respectively.

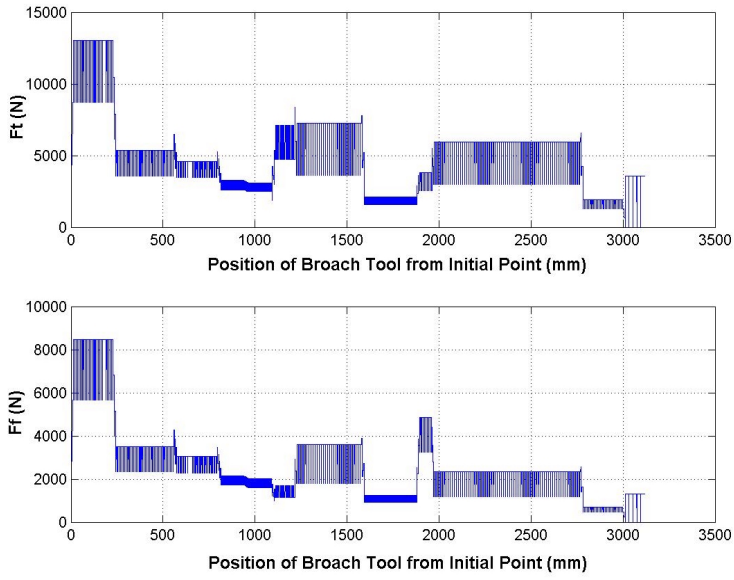

Figure 5-1: Cutting Force predictions after modifications.

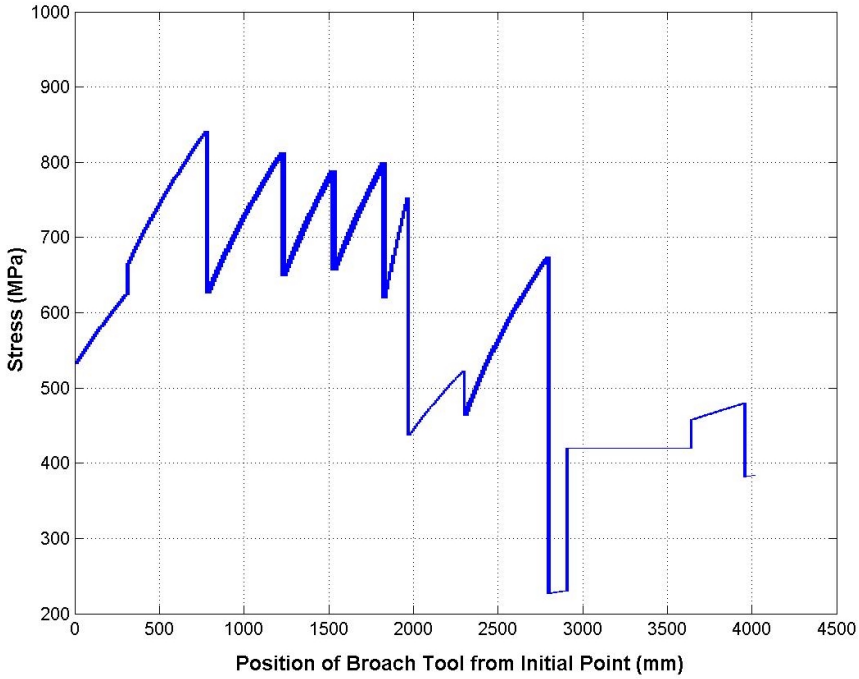

Figure 5-2: Tooth Stress prediction after modification.

The improvements can be summarized in Table 5-2

		Before	After
Broach Tool Length (mm)		4122	3128
Form error (μm)		29.2	26.5
Max. Tooth Stress (MPa)		730	840
Chip Space Percentage (%)		27	29
Force Fluctuations between sections (%)	Ft	276	131
	Ff	429	300

Table 5-2: Improvements in broach design.

5.2 Broach Tool Optimization Problem

Another method is formulating the problem by constructing a mathematical model to represent the broaching process. As mentioned before the aim is to maximize the material removal rate. In broaching, there are several constraints which can be summarized as tooth breakage, machine power, ram length of the machine and part quality. These constraints are discussed in detail in Chapter 2 and Chapter 3 and summarized in the following sections.

In order to optimize the broaching process problem, the objective function and the constraints can be summarized as follows.

The material removal rate can be calculated as;

$$MRR = \frac{Volume\ removed}{time}$$

The volume removed per one tooth, $V_{pt,}$ can be expressed as;

$$V_{pt} = wt_i b_i$$

then, the total volume removed is

$$V_{total} = w\sum_{i:1}^{N_s} t_i b_i n_i \quad i{:}1,..,N_s$$

where N_s is the number of sections, n_i is the number ot teeth in the i^{th} section

The process time can be calculated as

$$time = \frac{distance}{velocity} = \frac{w + \sum_{i:1}^{N_s} (n_i - 1) p_i}{V}$$

Then the objective function can be expressed as

$$\textbf{\textit{Objective function:}}\ \text{Max}\quad MRR = \frac{w\sum_{i:1}^{N_s} t_i b_i n_i}{w + \sum_{i:1}^{N_s} (n_i - 1) p_i} V \tag{5.1}$$

The constraints can be defined as follows;

Subject to:

1. **Total Tool length**

$$\sum_{i=1}^{N_s} (n_i - 1) p_i \le \textit{Available Machine Ram Length} \tag{5.2}$$

where p_i is the pitch (distance between two successive teeth)

2. **Power**

In order to calculate the power, first of all tangential cutting forces created by teeth in-cut have to be calculated.

Total tangential cutting forces in section *i* can be calculated from;

$$F_{total,i} = m\left(K_{tc} t_i b_i + K_{te} b_i\right)$$

where *m* is the number of teeth in-cut.

$m_i = ceil(\frac{w}{p_i})$ where ceil is the function that rounds the expression to the nearest upper integer.

The total power has to be less than the available power of the machine;

$$F_{total,i} V < \textit{Available Machine Power} \tag{5.3}$$

3. **Tooth Stress**

The resultant cutting force on one teeth F_i;

$$F_i = \sqrt{Ft_i^2 + Ff_i^2}$$

$$Ft_i = K_{tc} t_i b_i + K_{te} b_i$$

$$Ff_i = K_{fc} t_i b_i + K_{fe} b_i$$

So the tooth stress is

- $S_i = F_i(1.3H_i^{0.374}B_i^{-1.09}T_i^{0.072}A_i^{0.088}R_{1i}^{-0.082}l_i^{-0.356}) \le Permissible\ Stress$ (5.4)
-

4. Chip Space

Chip jam is a common problem in broaching. Broach chips can be very short depending on the thickness of the part. If there is not enough curvature in the chip they may get stuck on the surface. This is usually overcome by using brush on the teeth. Another problem is the chip space. If there is not enough space in the gullet, chips may get stuck in that space and cause jamming.

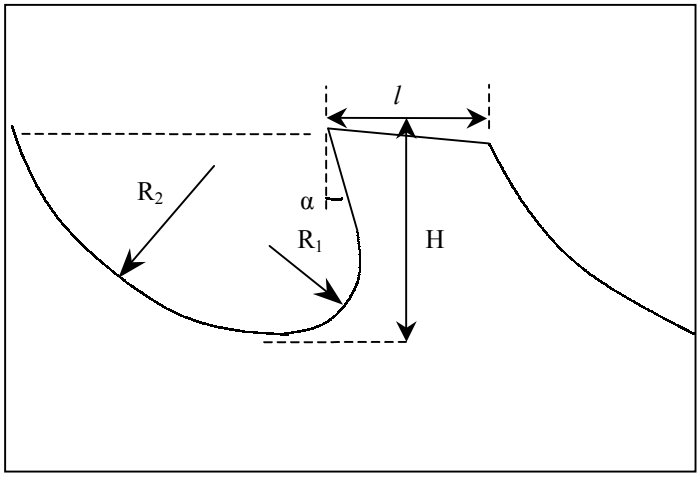

Figure 5-3: Gullet area definition.

The space in the gullet has to be checked for sufficient chip room. For this purpose, an equation is developed as:

$$GA=0.9456(p-l)^{0.816}H^{1.14}R_1^{0.026}R_2^{-0.0891}\alpha^{0.0388} \quad (5.5)$$

where all dimensions are in (mm) and α is in (deg) (Figure 5-3).

A test matrix is formed as in Table 5-3 in order to consider the effects of parameters to the gullet area. Each parameter is varied by keeping the others constant. Then each case is drawn in Catia v5r8 and the gullet area is measured. Finally, the gullet area is fitted to an equation. The differences between the values obtained from the equation (5.5) and the measured values are acceptable.

The cut chip volume can be calculated as

$V_{pt,i} = wt_ib_i$

and the gullet space of teeth in each section ;

$V_{Gullet,i} = 0.9456w(p_i - l_i)^{0.816}H_i^{1.14}R_{1i}^{0.026}R_2i^{-0.0891}A_i^{0.0388}$

As described before, gullet space is critical for chip jamming. There has to be sufficient space for chips in the gullet area. This is recommmended as 2-4 times of the chip volume. Monday[23].

$$\frac{V_{pt,i}}{V_{Gullet,i}} \leq 0.35$$

$$\frac{wt_i b_i}{0.9456w(p_i - l_i)^{0.816} H_i^{1.14} R_{1i}^{0.026} R_{2i}^{-0.0891} A_i^{0.0388}} \leq 0.35 \tag{5.6}$$

(P-L) (mm)	H (mm)	R_1 (mm)	R_2 (mm)	α (°)	Gullet Area (mm^2)	Fitted Gullet Area (mm^2)	Error (%)
5,58	3,96	1,98	7,95	12	17,2	17,2	0,1
4,00	3,96	1,98	7,95	12	14,3	13,1	8,3
5,00	3,96	1,98	7,95	12	16,0	15,7	1,6
6,00	3,96	1,98	7,95	12	18,2	18,3	0,5
7,00	3,96	1,98	7,95	12	20,9	20,7	0,8
5,58	3,50	1,98	7,95	12	14,8	14,9	0,7
5,58	3,00	1,98	7,95	12	12,4	12,5	1,5
5,58	2,50	1,98	7,95	12	9,9	10,2	2,5
5,58	4,50	1,98	7,95	12	20,0	19,9	0,6
5,58	5,00	1,98	7,95	12	22,8	22,4	1,3
5,58	6,00	1,98	7,95	12	28,5	27,6	3,0
5,58	3,50	2,50	7,95	12	15,5	15,0	3,1
5,58	3,50	1,50	7,95	12	14,5	14,8	2,5
5,58	3,50	1,00	7,95	12	14,3	14,7	3,0
5,58	3,50	0,50	7,95	12	14,1	14,4	2,3
5,58	3,96	1,98	7,50	12	17,3	17,3	0,2
5,58	3,96	1,98	7,00	12	17,4	17,4	0,3
5,58	3,96	1,98	6,50	12	17,5	17,5	0,4
5,58	3,96	1,98	6,00	12	17,6	17,7	0,3
5,58	3,96	1,98	5,50	12	17,8	17,8	0,1
5,58	3,96	1,98	5,00	12	18,0	17,9	0,5
5,58	3,96	1,98	4,50	12	18,4	18,1	1,5
5,58	3,96	1,98	4,00	12	19,0	18,3	3,6
5,58	3,96	1,98	8,50	12	17,1	17,1	0,1
5,58	3,96	1,98	9,00	12	17,1	17,0	0,3
5,58	3,96	1,98	9,50	12	17,0	16,9	0,5
5,58	3,96	1,98	7,95	10	17,1	17,1	0,1
5,58	3,96	1,98	7,95	5	16,9	16,6	1,6
5,58	3,96	1,98	7,95	30	18,0	17,8	0,8
5,58	3,96	1,98	7,95	45	18,1	18,1	0,2
5,00	3,50	1,50	7,00	12	13,3	13,7	2,9
5,00	3,50	1,50	7,00	5	13,0	13,3	1,7
5,00	3,50	1,50	7,00	30	14,2	14,2	0,2
5,00	3,50	1,50	7,00	20	13,7	14,0	2,2
4,00	2,00	0,50	7,00	15	5,6	5,9	5,9
4,00	2,00	0,50	4,00	15	6,5	6,2	4,0
6,38	1,98	0,51	11,10	15	9,0	8,2	8,9

Table 5-3: Gullet Area.

5. Chip load

The chip load has limitations in order to prevent rubbing or chipping.

$$t_i \geq 0.012 \text{ to avoid rubbing}$$
$$t_i \leq 0.065 \text{ to avoid chipping} \tag{5.7}$$

6. Number of teeth

The necessary number of teeth can be calculated according to previous design. Since the amount of chip cut by current design has to be same with the new optimal design;

(Current number of teeth)$_i$ (current chip load)$_i$ = n_i t_i

$$(n_c)_i (t_c)_i = n_i t_i \tag{5.8}$$

7. Tooth Geometry

As the pitch decreases or increases because of the machinability constraints, the height, land and gullet radius have to change accordingly accomodate the change in the pitch. So, these parameters are related to the pitch with some constants defined as follows.

$$H_i = c_{1i} p_i$$
$$R_{1i} = c_{2i} p_i$$
$$R_{2i} = c_{3i} p_i \tag{5.9}$$
$$l_i = c_{4i} p_i$$

The *c* constants are calculated according to the current design and they must be selected according to the manufacturability constraints and the smooth chip flow.

8. Additional constraints due to practical considerations

The pitch is kept between some reasonable values as

$$5 \leq p_i \leq 12 \tag{5.10}$$

The land length is kept smaller than the pitch

$$l_i \leq p_i \tag{5.11}$$

9. Manufacturability of the improved tool design

The manufacturability of broach tools may impose other constraints. Since most of the sections are manufactured by standart tools, an extraordinary design will be time consuming and will lead to increased cost. For example a broach design with variable pitch or rise in the same section may suppress chatter, improve surface finish and tool life, but it may also increase manufacturing and resharpening cost. For most of the tools, the gullet radius (R_1) in a section is the same for easy grinding of the tool. For this reason, it is important to consider manufacturability of the improved tool design before it is implemented.

5.3 Mathematical Modeling of Optimization Problem

The mathematical representation of the broaching optimization problem can be written as the following.

Model:

$$\text{Obj: } Max\ MRR = \frac{w\sum_{i:1}^{N_s} t_i b_i n_i}{w + \sum_{i:1}^{N_s} (n_i - 1) p_i} V$$

Decision variables:

t_i:chip load

n_i: number of teeth in a section

p_i: pitch of the section

Variables:

H_i: heigth of the tooth

B_i:Width of the tooth

T_i: Top length of the tooth

A_i: Angle of the tooth

$(R_1)_i$: Gullet radius

$(R_2)_i$: Pre-gullet radius

l_i: Land length

Constants

w: part thickness

N_s: number of sections

V: Cutting speed

$K_{tc}, K_{te}, K_{fc}, K_{fe}$: Cutting constants

Parameters

b_i: chip width

$(n_c)_i$: Current number of teeth

$(t_c)_i$: Current chip thickness

c_1, c_2, c_3, c_4 : pitch related constants

S.t.: $\sum_{i=1}^{N_s}(n_i - 1)p_i \le 5000$

$$m\left(K_{tc}t_i b_i + K_{te}b_i\right)V < 3000$$

$$m = \frac{w}{p} + 1$$

$$\sqrt{(K_{tc}t_i b_i + K_{te}b_i)^2 + (K_{fc}t_i b_i + K_{fe}b_i)^2}\,(1.3H_i^{0.374}B_i^{-1.09}T_i^{0.072}A_i^{0.088}R_{1i}^{-0.082}l_i^{-0.356}) \le 750$$

$$\frac{wt_i b_i}{0.9456w(p_i - l_i)^{0.816}H_i^{1.14}R_{1i}^{0.026}R_2 i^{-0.0891}A_i^{0.0388}} \le 0.35$$

$$t_i \ge 0.012$$

$$t_i \le 0.065$$

$$(n_c)_i \; x \; (t_c)_i \; = \; n_i \; x \; t_i$$

$$H_i = c_{1i}p_i$$

$$R_{1i} = c_{2i}p_i$$

$$R_{2i} = c_{3i}p_i$$

$$l_i = c_{4i}p_i$$

$$5 \le p_i \le 12$$

$$l_i \le p_i$$

The optimization of the broaching process defined above is a problem requires constraint nonlinear programming methods. Both the objective function and some of the constraints are nonlinear. Nonlinear programming techniques are mathematically advanced and conceptually difficult [40]. They require some fluency in differential calculus and linear algebra. The constraints are too complex to find a unique minimum and feasible regions that have nonlinear boundaries and that are non-convex. Also it is almost impossible to find the optimal solution in nonlinear problems.

The mathematical model in section 5.3 is coded in GAMS[4]. The solvers CONOPT and MINOS are used but the solvers cannot find a feasible solution. This means there is no a feasible solution. The problem is the method the solvers use. The CONOPT solver uses the reduced gradient method to find the optimal solution. The MINOS employs a project Lagrangian algorithm. This involves a sequence of major iterations, each of which requires the solution of a linearly constrained sub problem. Each sub problem contains linearized versions of the nonlinear constraints, as well as the linear constraints and bounds.

5.4 Summary

In this chapter, the improvement in broach tool design is achieved by using the models obtained in previous chapters. It is shown that significant improvements could be obtained using the obtained models. Also optimization by using GAMS software is tried to be done but the software could not find a feasible solution for the problem.

[4] GAMS is a registered trade mark of GAMS Software GMBH. The General Algebraic Modeling System (GAMS) is a high-level modeling system for mathematical programming problems. It consists of a language compiler and a stable of integrated high-performance solvers.

CHAPTER 6 DISCUSSION AND CONCLUSION

Broaching is used in variety of applications and can provide high productivity and part quality. Tool design is the most critical aspect of broaching as the cutting conditions are set by the broach geometry which cannot be modified during the process. The limitations such as tooth breakage, machine power, part quality, tool wear are modeled in order to improve the process.

There are number of constraints which have to be respected in optimization of the tool design. Cutting loads must be limited according to the available machine power and tooth breakage limit. The force fluctuations must be minimized to eliminate quality problems and accelerated tool wear. Deflections must be limited for tolerance integrity of the part. These and similar other constraints considered in optimization of the chip thickness or rise per tooth and the pitch.

In this study, as a first step process is modeled. Force model is obtained by using several methods such as mechanistic models, finite element analysis and experimental methods. Using force model, power model is obtained. It is seen that power obtained by using the experimental force model correlates to the power monitoring results [30] reasonably well. FEA model does not correlate very well but the effects of parameters are helpful. Also a model for chatter stability for broaching process is presented. Then structural modeling of the process is done. A parametric tooth stress formulation for generalized tooth geometry is obtained by FEA since it is hard to obtain it analytically. Also the final part shape is generalized and equations are obtained by FEA for part deflections in order to calculate the form errors. The equation obtained for the part deflection considers the force application location which is hard to calculate analytically

and the algorithm used for calculation of form error considers the change in the geometry.

A simulation system is implemented for prediction of cutting forces, power, and tooth stress and part deflections. The program provides predictions for a given work material and tool geometry. Tool design can be improved based on the predictions which is demonstrated by an example. As an application, a current tool design for fir-tree profile production is improved by varying chip load and pitch and using obtained models and significant improvements are observed.

As a future work the optimization of the broaching will be improved by using nonlinear optimization techniques. An optimization program can be coded using one of the proper algorithms for constrained nonlinear programming. Also the simulation program can be written as more user friendly.

In this thesis, a complete broaching model is obtained for optimization purposes which is not present in the literature. It is seen that by using the models obtained in this thesis the process efficiency can be improved. This thesis forms a basis for the next studies in improvement and optimization of broaching process.

REFERENCES

1 Taylor, F.W, 1907, On the Art of Cutting Metals, ASME Trans, 28:31-350.

2 Armerago, E.J.A. and Brown, R.H., 1969, The Machining of Metals. Prentice-Hall.

3 Shaw, M.C., 1984, Metal Cutting Principles. Oxford University Press.

4.Oxley, P.L.B, 1989, The Mechanics of Machining. Ellis Horwood Limited.

5 Altintas, Y., 2000, Manufacturing Automation: metal cutting mechanics, machine tool vibrations and CNC design, Cambridge University Press.

6 Trent, E.M. and Wright, P.K., 2000, Metal Cutting, Butterworth-Heinemann.

7 Childs, T.H.C., Maekawa, K., Obikawa, T., Yamane, Y., 2000, Metal Machining Theory and Applications, Arnold Publishers.

8 Merchant, M.E., 1945, Mechanics of metal cutting process, J. Appl. Phys. 16:318-324,

9 Lee, E.H. and Shaffer, B.W., Theory of Plasticity Applied to the Problem of Machining, Journal of Applied Mechanics.

10 Palmer, W.B. and Oxley, P.L.B, 1963, Mechanics of Orthogonal Machining. Proceedings Instituition of Mechanical Engineers, 177:789-802.

11 Krystof, J., 1939, Berichte uber Betriebswissenschafliche Arbeiten, Bd., 12. VDI Verlag.

12 Zienkiewicz, O.C., 1971, The Finite Element Method in Engineering Science 2nd edn. Ch. 18, Mc Graw Hill, London.

13 Kakino, Y., 1971, Analyses of the mechanism of orthogonal maching by finite element method, J.Japan Soc. Prec. Eng. 37/7: 503-508.

14 Shirakashi, T. and Usui, E., 1976 Simulatioon analyses of orthogonal metal cutting processes, J. Japan Soc. Pres. Eng. 42/5: 340-345.

15 Iwata, K., Osakada, K. and Terasaka, 1984, Y. Process modeling of orthogonal cutting by rigid-plastic finite element method, Trans ASME J. Eng. Mat. Tech., 106:132-138.

16 Strenkowski, J.S. and Carol III, J.T., 1985, A finite element model of orthogonal metal cutting, Trans ASME J. Eng. Ind. 107:349-354.

17 Maekawa, K., Ohhata, H. and Kitagawa, T, 1994, Simulation analyses of cutting performance of a three-dimensional cut-away tool. In Usui, E. (ed.), Advencement of Intelligent Production. Tokyo: Elsevier, 378-283.

18 Ueda, K. and Manabe, K., 1993, Rigid-plastic FEM Analyses of three-dimensional deformation field in chip formation process, Annals of CIRP, 42/1: 35-38.

19 Ueda, K., Manabe, K. and Nozaki, S., 1996, Rigid-plastic FEM of three-dimensional cutting mechanism (2nd report) – simulation of plain milling process, J. Japan Soc. Prec. Eng., 62/4: 526-531.

20 Sekhon, G.S. and Chenot, S., 1993, Numerical Simulation of continuos chip formation during non-steady orthogonal cutting, Engineering Computations, 10:31-40.

21 Ceretti, E., Fallbohmer, P. Wu, W.T. and Altan T., 1996, Application of 2-D FEM to chip formation in orthogonal cutting, J. Materials Processing Tech., 59:169-181.

22 Marusich, T.D. and Ortiz, M., 1995, Modeling and Simulation of high speed machining, Int. J. Num. Methods in Engineering, 38: 3675-3694.

23 Monday, C., 1960, Broaching, The Machinery Publishing Co. Ltd.

24 Kokmeyer, E., 1984, Better Broaching Operations, Society of Manufacturing Engineers.

25 Terry, R.W., Karni, R. and Huang, Y-J., 1992, Concurrent Tool and Production System Design For a Surface Broach Cutting Tool: A Knowledge-Based Systems Approach, International Journal of Production Research, 30/2 :219-240.

26 Gilormini, P., Felder, E., 1984, A Comparative Analysis of Three Machining Processes: Broaching, Tapping and Slotting, Annals of the CIRP, 33/1:19-22.

27 Sutherland, J.W., Salisbury, E.J. and Hoge, F.W., 1997, A Model For the Cutting Force System In the Gear Broaching Process, International Journal of Machine Tools and Manufacture, 37/10 :1409-1421.

28 Sajeev, V., Vijayaraghavan, L. and Rao, U.R.K., 2000, Analysis of the Effects of Burnishing in Internal Broaching, International Journal of Mechanical Engineering Education, 28/2 :163-173.

29 Taricco, F., 1995, Effect of Machining and Shot Peening on the Residual Stresses of Superalloy Turbine Discs, ASME Paper 95-GT-366.

30 Budak, E., 2001, Broaching Process Monitoring, Proceeedings of Third International Conference on Metal Cutting and High Speed Machining, Metz-France, 251-260.

31 Bhattacharya, A., Faria-Gionzalez, R., and Ham, I., 1970, Regression analysis for predicting surface finish and its application in the determination of optimum machining conditions, ASME Journal of Engineering for Industry, Transactions, 92/:711-714.

32 Ermer, D.S., 1971, Optimization of the constrained machining economics problem by geometric programming, ASME Journal of Engineering for Industry, 93:1067-1072.

33 Satyanarayana, B., Rao, P.N. and Tewari, N.K., 1986, Application of non-linear goal programming technique in metal cutting, Proc. the 12th All India Machine Tool Design and Research Conf., liT Delhi, India, 483-486.

34 Arsecularatne, J.A., Hiduja, S. and Barrow, G., 1992, Optimum cutting conditions for turned components, Proc. Inst. Mech. Engrs., 206/B2:15-31.

35 Mesquita, R., Krastera, E. and Doytchinov, S., 1995, Computer-aided selection of optimum machining parameters in multipass turning, Int. J. Adv. Manuf. Technol., 10:19-26.

36 Khan, Z., Prasad, B., and Singh, T., 1997, Machining condition optimization by Genetic Algorithms and Simulated Annealing, Computers Ops. Res., 24:7: 647-657.

37 Alberti, N. and Perrone, G., 1999, Multipass machining optimization by using fuzzy possibilistic programming and Genetic Algorithms, Proc. Instn. Mech. Engrs., 213 /B: 261-273.

38 Budak, E., Altintas, Y and Armerego, E.J., 1996, Prediction of Milling Force Coefficients from Orthogonal Cutting Data, Trans. ASME Journal of Manufacturing Science and Engineering. 18:216-224.

39 Koenigsberger, F. and Tlusty, J., 1967, Machine Tool Structures-Vol. I: Stability Against Chatter, Pergamon Press.

40 Daellenbach, H.G. , George, J.A. , McNickle, D.C., 1983, Intoduction to Operations Research Techniques, Allyn and Bacon, Inc

41 Timoshenko, S., MacCullough G.H., 1949, Elements of Strength of Materials, D. Van Nostrand Company, Inc.

REFERENCES

1 Taylor, F.W, 1907, On the Art of Cutting Metals, ASME Trans, 28:31-350.

2 Armerago, E.J.A. and Brown, R.H., 1969, The Machining of Metals. Prentice-Hall.

3 Shaw, M.C., 1984, Metal Cutting Principles. Oxford University Press.

4.Oxley, P.L.B, 1989, The Mechanics of Machining. Ellis Horwood Limited.

5 Altintas, Y., 2000, Manufacturing Automation: metal cutting mechanics, machine tool vibrations and CNC design, Cambridge University Press.

6 Trent, E.M. and Wright, P.K., 2000, Metal Cutting, Butterworth-Heinemann.

7 Childs, T.H.C., Maekawa, K., Obikawa, T., Yamane, Y., 2000, Metal Machining Theory and Applications, Arnold Publishers.

8 Merchant, M.E., 1945, Mechanics of metal cutting process, J. Appl. Phys. 16:318-324,

9 Lee, E.H. and Shaffer, B.W., Theory of Plasticity Applied to the Problem of Machining, Journal of Applied Mechanics.

10 Palmer, W.B. and Oxley, P.L.B, 1963, Mechanics of Orthogonal Machining. Proceedings Instituition of Mechanical Engineers, 177:789-802.

11 Krystof, J., 1939, Berichte uber Betriebswissenschafliche Arbeiten, Bd., 12. VDI Verlag.

12 Zienkiewicz, O.C., 1971, The Finite Element Method in Engineering Science 2nd edn. Ch. 18, Mc Graw Hill, London.

13 Kakino, Y., 1971, Analyses of the mechanism of orthogonal maching by finite element method, J.Japan Soc. Prec. Eng. 37/7: 503-508.

14 Shirakashi, T. and Usui, E., 1976 Simulatioon analyses of orthogonal metal cutting processes, J. Japan Soc. Pres. Eng. 42/5: 340-345.

15 Iwata, K., Osakada, K. and Terasaka, 1984, Y. Process modeling of orthogonal cutting by rigid-plastic finite element method, Trans ASME J. Eng. Mat. Tech., 106:132-138.

16 Strenkowski, J.S. and Carol III, J.T., 1985, A finite element model of orthogonal metal cutting, Trans ASME J. Eng. Ind. 107:349-354.

17 Maekawa, K., Ohhata, H. and Kitagawa, T, 1994, Simulation analyses of cutting performance of a three-dimensional cut-away tool. In Usui, E. (ed.), Advencement of Intelligent Production. Tokyo: Elsevier, 378-283.

18 Ueda, K. and Manabe, K., 1993, Rigid-plastic FEM Analyses of three-dimensional deformation field in chip formation process, Annals of CIRP, 42/1: 35-38.

19 Ueda, K., Manabe, K. and Nozaki, S., 1996, Rigid-plastic FEM of three-dimensional cutting mechanism (2nd report) – simulation of plain milling process, J. Japan Soc. Prec. Eng., 62/4: 526-531.

20 Sekhon, G.S. and Chenot, S., 1993, Numerical Simulation of continuos chip formation during non-steady orthogonal cutting, Engineering Computations, 10:31-40.

21 Ceretti, E., Fallbohmer, P. Wu, W.T. and Altan T., 1996, Application of 2-D FEM to chip formation in orthogonal cutting, J. Materials Processing Tech., 59:169-181.

22 Marusich, T.D. and Ortiz, M., 1995, Modeling and Simulation of high speed machining, Int. J. Num. Methods in Engineering, 38: 3675-3694.

23 Monday, C., 1960, Broaching, The Machinery Publishing Co. Ltd.

24 Kokmeyer, E., 1984, Better Broaching Operations, Society of Manufacturing Engineers.

25 Terry, R.W., Karni, R. and Huang, Y-J., 1992, Concurrent Tool and Production System Design For a Surface Broach Cutting Tool: A Knowledge-Based Systems Approach, International Journal of Production Research, 30/2 :219-240.

26 Gilormini, P., Felder, E., 1984, A Comparative Analysis of Three Machining Processes: Broaching, Tapping and Slotting, Annals of the CIRP, 33/1:19-22.

27 Sutherland, J.W., Salisbury, E.J. and Hoge, F.W., 1997, A Model For the Cutting Force System In the Gear Broaching Process, International Journal of Machine Tools and Manufacture, 37/10 :1409-1421.

28 Sajeev, V., Vijayaraghavan, L. and Rao, U.R.K., 2000, Analysis of the Effects of Burnishing in Internal Broaching, International Journal of Mechanical Engineering Education, 28/2 :163-173.

29 Taricco, F., 1995, Effect of Machining and Shot Peening on the Residual Stresses of Superalloy Turbine Discs, ASME Paper 95-GT-366.

30 Budak, E., 2001, Broaching Process Monitoring, Proceeedings of Third International Conference on Metal Cutting and High Speed Machining, Metz-France, 251-260.

31 Bhattacharya, A., Faria-Gionzalez, R., and Ham, I., 1970, Regression analysis for predicting surface finish and its application in the determination of optimum machining conditions, ASME Journal of Engineering for Industry, Transactions, 92/:711-714.

32 Ermer, D.S., 1971, Optimization of the constrained machining economics problem by geometric programming, ASME Journal of Engineering for Industry, 93:1067-1072.

33 Satyanarayana, B., Rao, P.N. and Tewari, N.K., 1986, Application of non-linear goal programming technique in metal cutting, Proc. the 12th All India Machine Tool Design and Research Conf., liT Delhi, India, 483-486.

34 Arsecularatne, J.A., Hiduja, S. and Barrow, G., 1992, Optimum cutting conditions for turned components, Proc. Inst. Mech. Engrs., 206/B2:15-31.

35 Mesquita, R., Krastera, E. and Doytchinov, S., 1995, Computer-aided selection of optimum machining parameters in multipass turning, Int. J. Adv. Manuf. Technol., 10:19-26.

36 Khan, Z., Prasad, B., and Singh, T., 1997, Machining condition optimization by Genetic Algorithms and Simulated Annealing, Computers Ops. Res., 24:7: 647-657.

37 Alberti, N. and Perrone, G., 1999, Multipass machining optimization by using fuzzy possibilistic programming and Genetic Algorithms, Proc. Instn. Mech. Engrs., 213 /B: 261-273.

38 Budak, E., Altintas, Y and Armerego, E.J., 1996, Prediction of Milling Force Coefficients from Orthogonal Cutting Data, Trans. ASME Journal of Manufacturing Science and Engineering. 18:216-224.

39 Koenigsberger, F. and Tlusty, J., 1967, Machine Tool Structures-Vol. I: Stability Against Chatter, Pergamon Press.

40 Daellenbach, H.G. , George, J.A. , McNickle, D.C., 1983, Intoduction to Operations Research Techniques, Allyn and Bacon, Inc

41 Timoshenko, S., MacCullough G.H., 1949, Elements of Strength of Materials, D. Van Nostrand Company, Inc.